Characterization of bias-enhanced nucleation of diamond on silicon by *in vacuo* surface analysis and transmission electron microscopy

B. R. Stoner, G.-H. M. Ma, S. D. Wolter, and J. T. Glass
Department of Materials Science and Engineering, North Carolina State University, Raleigh, North Carolina 27695-7919
(Received 15 October 1991)

An in-depth study has been performed of the nucleation of diamond on silicon by bias-enhanced microwave plasma chemical vapor deposition. Substrates were pretreated by negative biasing in a 2% methane-hydrogen plasma. The bias pretreatment enhanced the nucleation density on unscratched silicon wafers up to 10^{11} cm^{-2} as compared with 10^{7} cm^{-2} on scratched wafers. *In vacuo* surface analysis including x-ray photoelecton spectroscopy (XPS), Auger electron spectroscopy, and combined XPS and electron-energy-loss spectroscopy were used to study systematically both the initial-nucleation and growth processes. High-resolution cross-sectional transmission electron microscopy (TEM) was used to study the physical and structural characteristics of the diamond-silicon interface as well as to complement and enhance the *in vacuo* surface-analytical results. Raman spectroscopy confirmed that diamond was actually nucleating during the bias pretreatment. Scanning electron microscopy has shown that once the bias is turned off, and conventional growth is conducted, diamond grows on the existing nuclei and no continued nucleation occurs. If the bias is left on throughout the entire deposition, the resulting film will be of much poorer quality than if the bias had been turned off and conventional growth allowed to begin. Intermittent surface analysis showed that a complete silicon carbide layer developed before diamond could be detected. High-resolution cross-sectional TEM confirmed that the interfacial layer was amorphous and varied in thickness from 10 to 100 Å. A small amount of amorphous carbon is detected on the surface of the silicon carbide and it is believed to play a major role in the nucleation sequence. A model is proposed to help explain bias-enhanced nucleation on silicon, in hopes that this will improve the understanding of diamond nucleation, in general, and eventually result in the nucleation and growth of better-quality diamond films.

I. INTRODUCTION

With its large band gap and a unique combination of properties, diamond is regarded as the most suitable candidate for many applications, ranging from wear-resistant coatings and optical windows for visible and infrared (ir) transmission to high-temperature electronic devices. Currently, diamond synthesis from the vapor phase under low pressure is routinely achieved by more than ten different methods. However, despite rapid progress, the mechanism(s) for diamond nucleation onto nondiamond substrates remains unknown. The understanding of nucleation phenomena appears to be essential for achieving heteroepitaxy of diamond, which is necessary for exploiting the potential of diamond electronic devices. It would also be extremely beneficial in controlling the microstructure and surface morphology of diamond coatings for various applications.

Since the time when diamond growth from the vapor phase was achieved at reasonable growth rates,[1–4] it has been a subject of argument as to whether diamond nucleation occurs in the gas phase (homogeneous nucleation) or on the substrate surface (heterogeneous nucleation). Fedoseev *et al.*[5–7] presented theoretical arguments, based on the classical nucleation theory, that homogeneous nucleation is possible. Furthermore, diamond powders have been collected directly from the gas phase,[8–12] which provides proof that such a nucleation process does exist. Nevertheless, the number of diamond particles collected from the gas phase was very small compared with the usual nucleation density (number of particles/cm^2) observed on a substrate surface. Furthermore, homogeneous-nucleation mechanisms cannot solely account for the large variety of nucleation densities observed on different substrate materials and that result from various surface pretreatments.

Several hypotheses for heterogeneous diamond nucleation onto foreign substrates have also been made, most of them based on experimental observation. It is well known that the diamond-nucleation density may be increased by several orders of magnitude by simply scratching or abrading the substrate surface prior to placing it into the growth chamber. Bachmann *et al.*[13,14] postulated that residual diamond particles left on the surface from the scratching medium acted as diamond-nucleation sites. This is based on the fact that diamond will tend to nucleate preferentially on the diamond seeds, thus resulting in discrete homoepitaxy of diamond. Recently, Iijima, Aikawa, and Baba[15,16] provided direct observation by high-resolution transmission electron microscopy (HRTEM) of diamond nucleation on "diamond seeds" left from the scratching process. However, abrading the substrate with nondiamond abrasives such as cubic boron nitride (cubic BN),[17] silicon carbide,[18] and stainless steel[19] has also yielded high nucleation densities. Furthermore, the diamond-nucleation density may be enhanced by nonabrasive surface pretreatments, such as the predeposition of carbonaceous layers of diamondlike carbon[20–22] (DLC) or even oil residue.[23,24] Another technique for nucleation enhancement, which has been employed in the experiments presented here and will be discussed in greater detail in a later section, is to simply bias the substrate negatively while immersed in a methane-hydrogen plasma.[25,26] Based on the variety of techniques used for the nucleation enhancement of diamond, presented above, it is the belief of the authors that the "diamond-seeding" hypothesis, although it has its merit and experimental evidence, is not the dominant mechanism for diamond nucleation from the gas phase.

Diamond nucleation is also favored on prominent features of the substrate surface, that is, surface morphologies that protrude with sharp edges or points, as opposed to valleys or flats. Such features are created by scratching or etching before or during the growth. Dennig and Stevenson[27,28] observed selected growth on chemically etched surfaces, and Kirkpatrick, Ward, and Economou[29] used sputtered crater arrays as a means of selected-area nucleation. It has been speculated that the total free energy of a diamond embryo is lowered by securing some minimized contact area with the substrate, thereby favoring a nucleation event at these morphological features. Since high diamond-nucleation densities can also be achieved with pretreatments that result in macroscopically smooth surfaces, such as with oil residues, it is believed that the "sharp-edge" mechanism should play a relatively minor role. Scratching is also believed to create a high surface-defect density, which will in turn act as favorable nucleation sites. However, despite extensive TEM work, to date there has been no direct observation to support this defect-related nucleation theory.

Experimental data suggest that diamond nucleation on nondiamond substrates is promoted by a stable carbonaceous precursor. This speculation is based on the fact that higher surface carbon concentration has been observed via both surface-[21,22,30,31] and bulk-sensitive techniques[32,33] on substrate surfaces pretreated with many of the nucleation-enhancing processes discussed above. The understanding of the nature and origin of such carbonaceous nucleation promoters created during a bias pretreatment is one of the major goals of the current research.

Interface chemistry was thought to play an important role in the diamond-nucleation process. Williams, Asbury, and Glass[34,35] observed an interfacial β-SiC layer between the silicon substrate and diamond film grown at 0.3% methane by cross-sectional TEM (XTEM) and again by x-ray photoelectron spectroscopy (XPS). Since then, carbide formation on various substrates has been observed prior to diamond nucleation and growth by many other researchers with electron and x-ray diffraction, as well as *in vacuo* surface-analytical techniques.[32–38] Joffreau, Haubner, and Lux[39,40] performed a systematic study of diamond growth on refractory metals (all are carbide formers) and observed that diamond nucleation occurred only after the formation of a thin carbide layer. They subsequently postulated that the difference in diamond-nucleation density, as observed on the various substrates, was related to the diffusivity of carbon in the respective carbide. However, attempts in the authors' laboratory to grow diamond on untreated bulk SiC substrates did not yield high nucleation densities, thus suggesting that carbide formation may only play an intermediate or secondary role. Others have reported favorable growth on SiC,[22,41] with nucleation densities only a few times greater than on untreated silicon. The importance of the carbide surface condition (order or disorder, stochiometric or nonstochiometric?) and the exact role that it plays in the promotion of diamond nucleation are thus unclear, although data presented in this study should help to alleviate some of this uncertainty.

Other noncarbide carbonaceous nucleation promoters have been postulated as well. Belton and co-workers observed, via *in vacuo* surface-analytical techniques, that diamond nucleation on platinum occurred on a surface that was mostly covered with a thin (1–3-monolayer) layer of hydrocarbons.[42,43] They also found that disordered graphite formed prior to diamond nucleation on a nickel substrate.[44] Angus *et al.* have also speculated that graphite may act as a diamond-nucleation precursor based on experiments where diamond nucleation was enhanced by the sprinkling of nonoriented graphite powders onto unscratched substrates.[45] Rudder *et al.* achieved a similar result from treating the surface with graphite fibers.[46] Ravi *et al.* observed that diamond nucleation could be enhanced by predepositing a layer of DLC in both combustion-flame and dc glow-discharge plasmas.[20,21] However, the actual nature of this DLC layer was never defined or well characterized, and other attempts to grow diamond on sputtered amorphous carbon and DLC have been unsuccessful in promoting high nucleation densities.[41,47] The discrepancy and diversity in the possible nucleation mechanisms presented above point to the need for a better understanding of the diamond-nucleation process. If the nature (structure and chemistry) and formation mechanism of this nucleation precursor can be identified, the nucleation of diamond from the vapor phase may then be more easily controlled and the deposition processes better tailored toward specific applications.

The purpose of the current research was to study systematically the nucleation of diamond on silicon enhanced via a predeposition biasing. To simplify and possibly reduce the number of active nucleation mechanisms, no *ex situ* pretreatments were employed. High nucleation densities on mirror-finished silicon were obtained via an *in situ* pretreatment that involves the deposition of an intermediate carbon layer by negatively biasing the substrate. Such a pretreatment method is very suitable for the study of diamond nucleation since it does not involve any scratching by diamond abrasives, therefore avoiding the confusion caused by the possibility of residual diamond seeds acting as nucleation sites. The chemical composition and structure of this intermediate carbon layer was characterized thoroughly via several *in vacuo* surface-analytical techniques including XPS, Auger electron spectroscopy (AES), and surface electron-energy-loss spectroscopy (EELS), as well as high-resolution XTEM, scanning electron microscopy (SEM), and Raman spectroscopy. The information presented in this study should significantly improve the current understanding of the diamond-nucleation process by providing strong evidence of a dominant diamond-nucleation mechanism under the conditions employed.

II. EXPERIMENTAL DETAILS

A. *In vacuo* chemical-vapor-deposition and analytical chambers

All samples used in this study were both grown and analyzed in the *in vacuo* chemical-vapor-deposition (CVD) and surface-analytical chamber shown in Fig. 1. This apparatus consists of a microwave plasma CVD reactor (A in Fig. 1) and a multitechnique surface-analytical chamber (B in Fig. 1) that are joined via a transfer tube (C in Fig. 1). All samples are initially introduced into the system via a central load lock (D in Fig. 1), which is isolated from the transfer tube via a gate valve and may be evaluated to 5×10^{-8} Torr by a separate turbopump. With this arrangement the samples may be transferred back and forth between the CVD and analytical chambers without being exposed to atmospheric contamination.

The microwave plasma CVD reactor (A in Fig. 1) consists of a 6-in.-inner-diameter stainless-steel chamber made by Applied Science Technology, Inc. (ASTeX) (A in Fig. 1). The power supply used was an ASTeX S-1000, 2.45-GHz microwave supply with a rectangular waveguide that is coupled to the cylindrical growth cavity. The substrate holder is a fully retractable, differentially pumped tantalum heater that may be used to control the substrate temperature independently of the plasma power. During processing, the growth chamber is pumped by a roots blower followed by a process mechanical pump. The chamber is ultrahigh vacuum (UHV) compatible and can be evacuated to a base pressure of 1×10^{-7} Torr by the attached turbopump. The substrate temperature is measured by an infrared pyrometer through a viewpoint normal to the substrate. The growth rate as well as the initial-nucleation process may be monitored *in situ* via laser-reflection interferometry (LRI).[25]

The analytical chamber (B in Fig. 1) is equipped with a Riber Mac2, semidispersive, electron analyzer which is used for both x-ray photoelectron spectroscopy and Auger electron spectroscopy. The x-ray source is a Riber dual-anode, Mg and Al, source. The electron source used for AES is a VG LEG61 electron gun, which is typically run at 3 kV and 200 μA emission. Acquisition of the XPS and AES spectra was achieved via an IBM PC/AT microcomputer. The XPS spectra for this study, obtained using Mg $K\alpha$, were acquired in the pulse-counting mode using a Riber pulse counter. For AES the analyzer was modulated at 8 kHz and the differential spectra were obtained using a lock-in amplifier.

B. Test of biasing effects on nucleation

The *in situ* biasing pretreatment is performed while the substrate is immersed in a methane-hydrogen plasma. Under standard growth conditions the holder-heater arrangement is isolated from ground (floating). The biasing pretreatment simply involves placing a negative dc bias (approximately 250 V) on the substrate relative to ground (Fig. 2). The substrate holder is approximately 1.5 in. in diameter, and the resulting current ranges from 100 to 200 mA. For a 1-cm^2 substrate, the resulting current flux is calculated to be approximately 15 mA/cm^2. The heater is a tantalum filament surrounded by, and isolated from, a welded 0.04-in.-thick tantalum can that is differentially pumped as described above. The sample holder is made of molybdenum and is designed to fit on the end of the tantalum can. The tantalum can is connected to a single feedthrough to which the dc bias is connected (Fig. 2).

C. Surface-analytical series versus bias time

This series was designed to observe systematically the nucleation process by intermittently stopping the bias pretreatment to study the chemical species on the surface. It has been previously documented that biasing

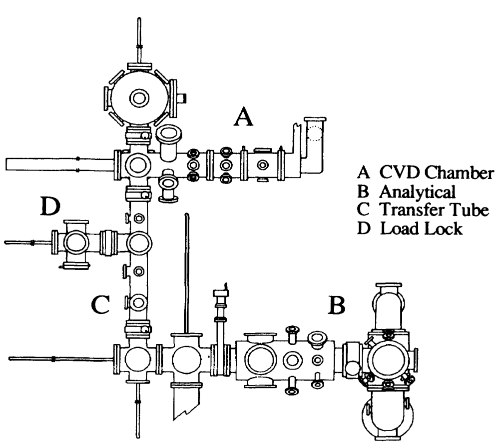

FIG. 1. *In vacuo* chemical-vapor-deposition and surface-analytical chamber.

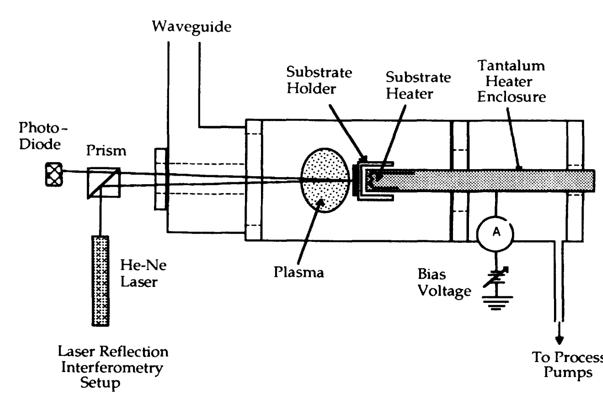

FIG. 2. CVD chamber showing *in situ* laser-reflection interferometry and substrate-biasing arrangements.

enhances the nucleation of diamond on silicon, yet the actual mechanism for this enhancement was not clearly understood. For this study a series of biasing pretreatments was interrupted at set intervals and then analyzed *in vacuo* to observe the changes in the surface chemistry that result. Table I outlines the experiments run and analyses performed for this pretreatment series.

From undoped silicon wafers, 1-cm^2 samples were prepared. They were subsequently ultrasonically cleaned in trichloroethylene (TCE), acetone, methanol, and 2-propanol and then rinsed in de-ionized (DI) water. Just prior to insertion into the load lock, they were dipped for 1 min into a 1:10 mixture of hydrofluoric acid in DI water to remove any existing native oxide, rinsed in DI water, and then blown dry with nitrogen. This procedure was designed to ensure minimal surface oxidation and hydrocarbon contamination on each of the samples used for this series.

The surface-analytical and biasing series was performed as follows. The substrates were biased at -250 V, immersed in a 2% methane in hydrogen plasma. The total flow rate was 1000 sccm, the net microwave power was maintained at 600 W, and the pressure was 15 Torr. Separate samples were biased for 1, 5, 15, 30, 60, 90, and 120 min. The plasma and bias were then shut off, the growth chamber was rapidly evacuated to 1×10^{-7} Torr, and the sample was subsequently transferred to the surface-analytical chamber. In the analytical chamber, XPS, XPS EELS, and AES were performed on each of the samples in this series. An as-inserted sample was also analyzed to observe the species present on the surface before the biasing pretreatment was initiated.

D. Analytical series versus growth time (after a 1-h bias)

The previous experimental series was designed to study the creation of nucleation sites. The present series was intended to observe and distinguish between the development of the nuclei and the growth of diamond on the existing sites. Table II outlines the experiments and analysis performed for this growth and analytical series.

The substrates were prepared identically to those in the preceding section. The samples were then biased for 1 h under the conditions described above. At the end of the biasing, the voltage was turned off, the bias leads were disconnected, leaving the substrate floating, the methane concentration was reduced to 1% at 1000 sccm of hydrogen, the pressure was increased to 25 Torr, and the substrate was moved to a distance of about 0.5 cm from the plasma. These experimental conditions are those that have been proven in the past to grow high-quality diamond films.[38] Samples were grown under these conditions for 0.75, 1.0, 2.0, and 5 h, the plasma was then turned off, the chamber pumped down, and the samples were transferred into the analytical chamber for surface analysis as described above.

E. Transmission electron microscopy

Cross-sectional transmission-electron-microscopy imaging in both conventional and high-resolution modes was used to confirm and expand on observations made by surface analysis via direct observation of nucleation sites and the resulting interface between the diamond and silicon. XTEM was performed on the samples that were biased for 1 and 2 h and then further grown for 5 h. Therefore the interface observed would represent that which was intermittently analyzed using XPS, AES, and XPS EELS during the growth series outlined above. It has been difficult to observe the actual nuclei in TEM because of low diamond-nucleation densities even by scratching pretreatments. Past observations may be inconclusive because the actual nucleation sites may not be included in the region of the TEM thin specimen examined. However, the present biasing pretreatment has made it possible to obtain very high nucleation densities; thus the probability of observing an actual diamond nuclei has been dramatically increased.

XTEM specimens were prepared by special mechanical thinning and ion-milling methods, described elsewhere.[48,49] The specimens were examined in a Philips EM 430 T analytical electron microscope (AEM) operated at 300 kV and in a Philips EM 400 AEM, which is equipped with a field-emission gun (FEG) and Gatan parallel-detection electron-energy-loss spectroscope, operated at 100 kV. High-resolution transmission electron microscopy was performed on a JEOL 4000 EX electron microscope operated at 400 kV, with a resolution of 1.8 Å.

TABLE I. Sample bias times and analysis performed during analytical series of nucleation during the biasing pretreatment.

	Analysis performed				
Bias time	XPS or AES	XPS EELS	Raman spectroscopy	SEM	TEM
Before bias	X				
1 min	X				
5 min	X	X			
15 min	X	X			
30 min	X	X		X	
1 h	X	X		X	
1.5 h	X	X	X	X	
2.0 h	X	X	X	X	

TABLE II. Sample bias or growth times and analysis performed during the analytical series study of growth after a bias pretreatment.

Bias or growth time (h/h)	Analysis performed XPS or AES	XPS EELS	Raman spectroscopy	SEM	TEM
1.0/0.0	X	X		X	
1.0/0.75	X	X			
1.0/1.0	X	X		X	
1.0/2.0	X	X		X	
1.0/5.0	X	X	X	X	X

III. RESULTS

A. Biasing results

Figure 3 shows SEM micrographs of diamond grown by microwave plasma CVD on (a) a Si wafer that was scratched with 0.25-μm diamond paste and (b) a pristine Si wafer that was pretreated by biasing. Both samples were further grown for 5 h under identical conditions. The Raman spectra from both the scratched and biased samples are shown in Fig. 4. The smaller diamond peak and larger background observed from the biased sample are indicative of films with higher nucleation densities and a larger number of grain boundaries.[50,51] The samples prepared by biasing were found to produce nucleation densities up to 10^{11} cm^{-2}, depending upon pretreatment time. This is contrasted with the scratched Si and pristine Si nucleation densities of 10^7 and 10^4 cm^{-2}, respectively. Nucleation on the untreated Si wafer was too low to measure, but a comparison with published nucleation densities of 10^3-10^5 cm^{-2} (Refs. 23 and 41) shows that the biasing technique has a pronounced affect on nucleation and is thus deserving of a more in-depth study.

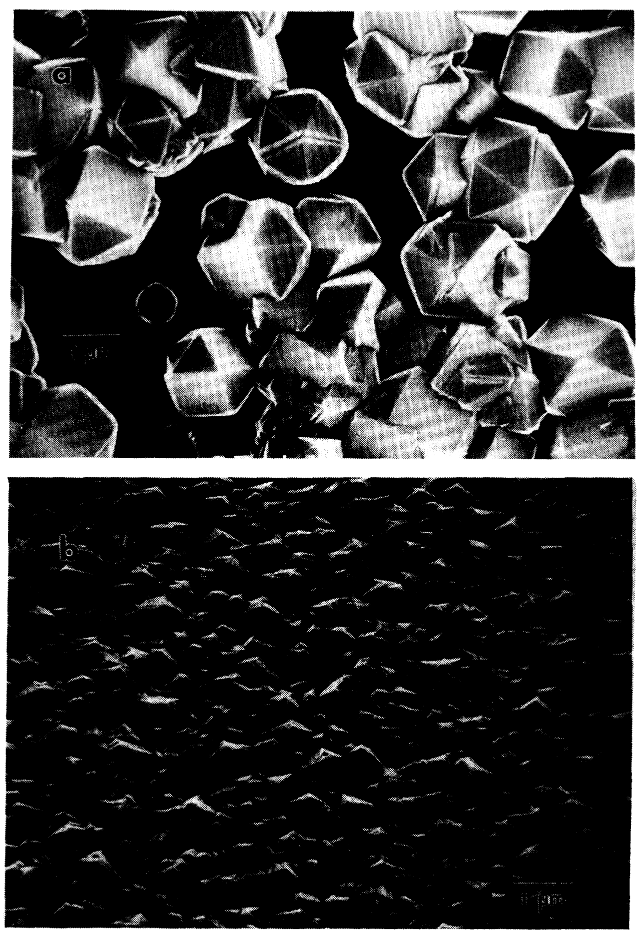

FIG. 3. SEM micrographs of samples grown under various pretreatments: (a) silicon wafer scratched with 0.25-μm diamond powder and (b) pristine silicon wafer biased on a (2% methane)-in-hydrogen plasma at -250 V for 1 h.

B. Surface-analytical series versus bias time

The carbon 1s core-level peak [Fig. 5(a)] was observed using XPS, as a function of bias time, of which the quantitative analysis is shown in Table III. The silicon substrate was found to have a small amount of carbon contamination on it before biasing began. This carbon contamination has been observed previously by other researchers[36–38] and was found, in the present experiments, to either be removed or converted into SiC in the first 5 min of biasing. From 5 min to 1 h the majority of

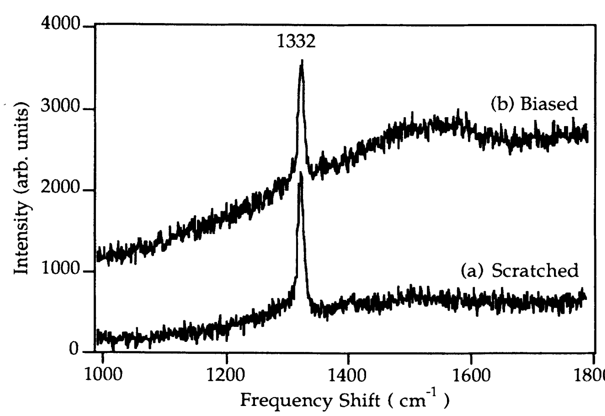

FIG. 4. Raman spectra of diamond grown on (a) scratched and (b) biased substrates shown in Figs. 3(a) and 3(b), respectively.

the carbon on the surface has a binding energy of 282.8 eV and is assigned to Si-C bonding. Deconvolution of the C 1s peaks shows that a smaller peak, approximately 20%, exists at 284.3 eV, which is characteristic of C-C bonding. The origin and structure of this excess C-C bonding is unclear as is its effect on the nucleation density.

It is unlikely that the C-C peak could represent diamond since such a large difference in nucleation density is observed (spanning several orders of magnitude) for biases of 5 min to 1 h. The fact that the relative percentage of this peak to the total C 1s is fairly constant at 20% for 5 min to 1 h suggests that it could be on the surface. In fact, a post-biasing sputter with argon in the analytical chamber was successful in removing the C-C, resulting in a single Si-C peak at 282.8 eV, thus confirming that this carbon was confined to the surface. The possible sources of this carbon could be any one or a combination of the following: (i) condensation of carbon from the hydrocarbon species in the gas phase when the plasma was turned off, (ii) carbon contamination from the walls of the CVD chamber, or (iii) an excess amount of carbon on the surface that is a direct result of the biasing process. The following experiments were performed to help determine the source of this surface carbon.

TABLE III. Quantification of species on the surface at various bias times as calculated from XPS peak-area ratios and relative sensitivity factors.

Bias time	Carbon 1s peak ratios $I_{\text{C-C}}:I_{\text{Si-C}}$	Silicon 2p peak ratios $I_{\text{Si-Si}}:I_{\text{Si-C}}$ $(:I_{\text{Si-O}})$	Concentration ratios [C]/[Si]
0.0 h	$(C_xH_yO_z)$	100:0	16:84
5 min	22:78	44:43:(13)	26:74
15 min	22:78	26:74	32:68
30 min	20:80	20:80	33:67
1 h	20:80	1:99	37:63
1.5 h	54:46	12:88	48:52
2.0 h	90:10	11:89	92:08

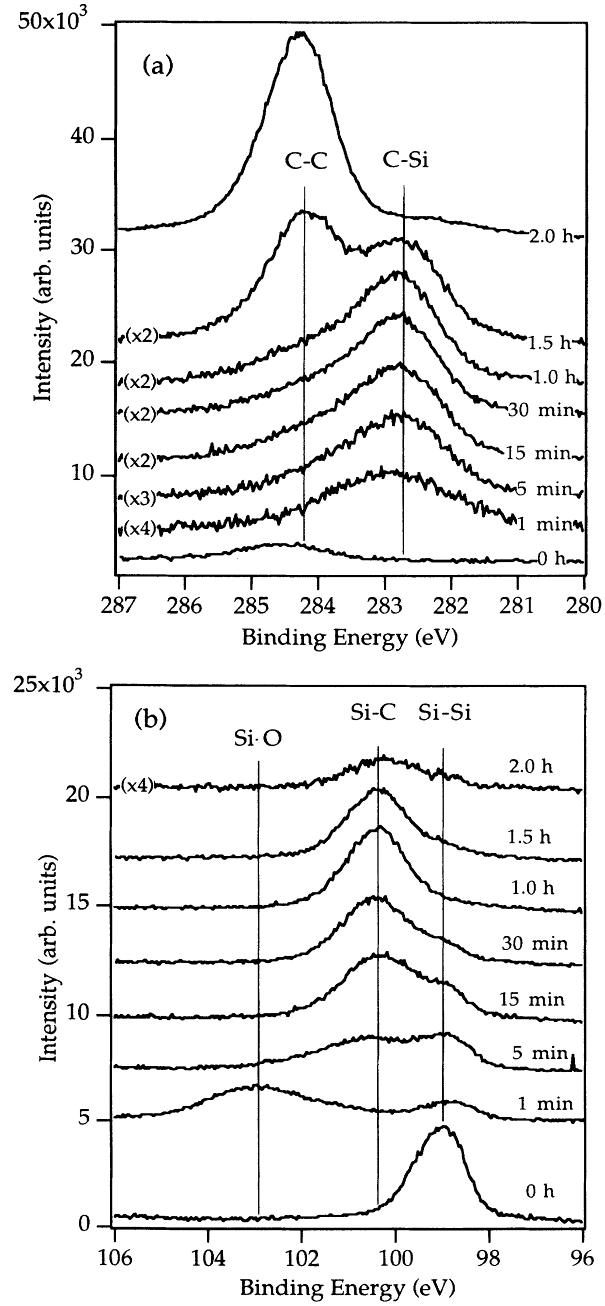

FIG. 5. XPS analysis as a function of bias-pretreatment time: (a) carbon 1s and (b) silicon 2p peak progressions.

When the plasma power is turned off, it is possible that carbon from the various hydrocarbon species present in the gas phase may then condense onto the substrate surface. To make sure that this condensation was not responsible for the excess carbon observed on the carbide surface, the methane flow was turned off following a 30-min bias, and the sample was exposed to a hydrogen plasma for 15 min. Surface analysis performed on this sample revealed that the substrate still contained elemental carbon in addition to silicon carbide, thus excluding the condensation of amorphous carbon from the gas phase as a possible source. Regarding item (ii), if contamination from the CVD chamber were a possible source of this carbon, an increase in the observed C-C contamination would be expected with increased exposure to the CVD chamber prior to analysis. For the samples observed in this study, the waiting time before analysis ranged from 15 min to 2 h and no dependence on this time was observed. This suggests that chamber contamination should be ruled out as a possible source. From these observations the authors propose that this small amount of carbon on the surface is caused by the biasing process, such as excess etching or sublimation of the Si from the Si-C or an increased flux of hydrocarbon ions to the surface. By exposing SiC to elevated temperatures, van Brommel, Crombeen, and Tooren showed, using low-energy electron diffraction (LEED) and AES, that the surface became carbon rich.[52] They speculated that this was due to the preferential evaporation of Si from SiC. In a hydrogen-rich plasma, it is possible that this process may be accelerated, resulting in the observed supersaturation of carbon on the substrate surface. This will be discussed further in Sec. IV A.

The Si 2p peak [Fig. 5(b)] was used to observe the chemical transformation of the silicon substrate as a function of bias time. Before biasing begins there exists only a single peak at 99.0 eV, which is representative of elemental silicon. After just 1 min of biasing, a majority of the silicon observed has been converted into silicon oxide (102.7 eV). By 15 min of biasing, however, the oxide has been totally removed and the resulting peak is a mixture of elemental silicon (99.0 eV) and Si-C (100.3 eV). From 15 min to 1 h of biasing, the Si-C peak steadily increases to nearly 100%, suggesting that it is covering the silicon substrate. At 1.5 h, corresponding to the sharp increase in the C 1s peak at 284.3 eV in Fig. 5(a), there is a reemergence of the elemental silicon signal at 99.0 eV. This suggests that etching of the interfacial SiC layer may be occurring, thereby bringing Si closer to the surface and causing an increase in the Si signal. By 2 h the C 1s peak shows over 90% C-C bonding, and the carbon-to-silicon ratio is up to over 90% as well, indicating that the surface is nearly covered with some elemental form of carbon. This elemental carbon is shown to be diamond by AES, XPS EELS, and Raman spectroscopy as presented in the following paragraphs.

The XPS series showed that a silicon film develops before the surface becomes covered with some elemental form of carbon. Overlayer calculations were performed on this carbide layer to determine its approximate thickness as a function of bias time. Calculations are based on an inelastic electron mean free path of 20 Å (Ref. 53) and assume a layer-by-layer growth model[54,55] of the silicon carbide overlayer for simplicity. The results of these calculations are shown in Table IV. Before biasing there exists a clean silicon substrate with approximately 4 Å of the amorphous and hydrogenated carbon on the surface. From 5 min to 1 h, the carbide thickness increases from approximately 10 to 90 Å, while the surface carbon increases slightly from 5 to 10 Å. At 1.5 h, concurrent with the observed increase in the elemental silicon peak, the carbide thickness drops drastically back down to approximately 45 Å and remains relatively unchanged by 2 h. Some preliminary biasing experiments performed on single-crystal SiC, in the authors' laboratory, have confirmed that SiC may be etched under the above conditions.

TABLE IV. Overlayer calculations for the biasing pretreatment, assuming an inelastic electron mean free path of 20 Å and a layered growth mode for the overlayer.

Bias time	Si-C layer thickness (Å)	C-C thickness (Å)	Si-O thickness (Å)
0.0 h		4	0
5 min	12	6	4
15 min	27	8	0
30 min	32	8	0
1 h	90	9	0
1.5 h	42	(diamond)	0
2.0 h	44	(diamond)	0

The layer-by-layer approximation used above may result in a low calculated value for the interfacial carbide thickness. If the carbide film at 1 h had a uniform thickness of 90 Å and the subsequent etching was nonuniform (i.e., islandlike), then the actual average thickness would be higher than the 45 Å calculated above. There would still be a decrease in the overall thickness from 1 to 1.5 h, but not as drastic. To calculate more accurately the actual layer thicknesses, one would have to assume a model that involved both layer-by-layer and island growth. One also would have to assume a fraction of the surface covered by the islands and a ratio of layered to island growth. So, in the above thickness calculations as well as those to follow, it is important to observe the qualitative trends and not the absolute thicknesses reported. A good review of overlayer-thickness calculations for electron spectroscopy may be found in Feldman and Mayer.[55]

Since the XPS core-level shifts can only provide chemical bonding information, C EELS and AES were implemented to help provide information as to the crystalline structure of the different forms of carbon observed on the surface during this series. Figures 6(a) and 6(b) display both standard AES and XPS-EELS spectra taken from natural type-IIA diamond, sputtered amorphous carbon, silicon carbide, and highly oriented pyrolytic graphite (HOPG). The AES fine structure from the bias-time series [Fig. 7(a)] indicates a transition from hydrogenated and amorphous carbon that exists on the surface before biasing begins to SiC by 30 min and then to diamond by 2 h of biasing. There is a subtle change from the 1-h-bias sample to the 1.5-h case, but without elaborate curve fitting the exact nature of this change is unclear.

From the XPS-EELS data [Fig. 7(b)], the transition from SiC to diamond is much more evident. From the standards shown in Fig. 6(b) and from previously published data,[37,56–58] silicon carbide has a characteristic bulk plasmon peak at 23 eV and diamond has both bulk and surface plasmon peaks at 35 and 25 eV, respectively. Diamond has also been shown to have a weak peak in the energy range from 14 to 17 eV, which is said to be due to interband transitions.[56,57] At 0.5 h the spectra clearly resembles that of SiC, with a single bulk-plasmon peak at 23 eV, and at 2 h resembles diamond with both bulk- and surface-plasmon peaks at 35 and 25 eV, respectively. However, at 1.5 h the spectra is a clear mixture of both diamond and SiC, thus suggesting that some diamond is present on the surface after 1.5 h of biasing. From this data it can be concluded that the sharp rise in the C 1s peak at 284.3 eV after 1.5 h of bias, shown in Fig. 5(a), was due to an increase in the number of diamond nuclei on the surface.

To further assure ourselves that the carbon observed after 1.5 and 2 h of bias was diamond, Raman spectroscopy was performed. Because of the relatively low Raman cross section for diamond, ten scans were performed and then subsequently superimposed in order to improve the signal-to-noise ratio. The carbon concentration on the 1.5-h sample was still too low to observe with this technique; however, the 2.0-h sample (Fig. 8) did produce a small characteristic diamond peak at 1332 cm^{-1}. No graphitic peaks were observed near 1580 cm^{-1}. Since graphite has about a 50 times higher Raman cross section than does diamond, it is highly improbable that the diamond could have nucleated on graphite. If it had nucleated on graphite, a Raman peak at 1580 cm^{-1} would have been observed for a nucleation density as high as that obtained here.

SEM micrographs were taken (Fig. 9) at 1-, 1.5-, and 2.0-h bias to see if the diamond could be observed. The 2-h sample showed that the surface was about 90% covered with diamond particles ranging in sizes from 10 to 60 nm in diameter (within the resolution of the Hitachi H-5000 field-emission microscope). The nucleation density from this sample was observed to be roughly 5×10^{10} cm^{-2}, with the understanding that there could be particles less than 10 nm in diameter that could not be observed because of the resolution limit of the microscope used. The 1.5- and 1.0-h samples showed decreasing nucleation densities, of particles within this same size range, of 5×10^{9} and 5×10^{8} cm^{-2}, respectively.

The 30-min sample had a very small number of observ-

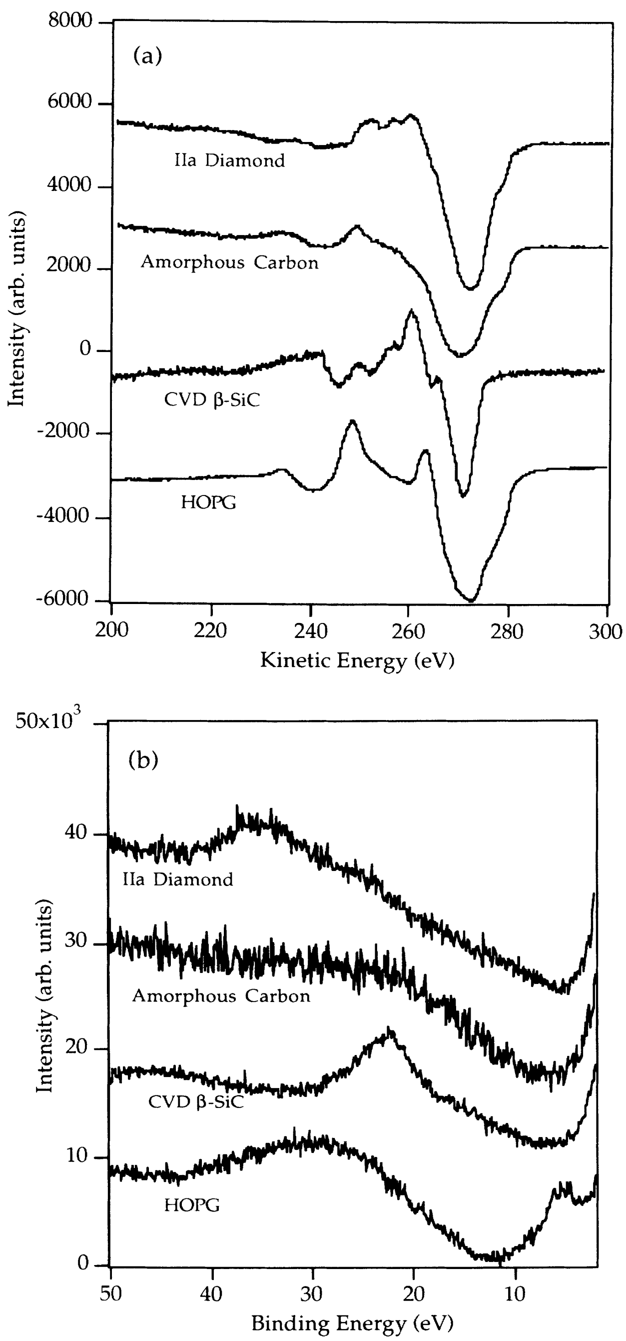

FIG. 6. Standard (a) AES and (b) XPS-EELS spectra from single-crystal diamond, amorphous carbon, single-crystal SiC, and highly ordered pyrolytic graphite (HOPG).

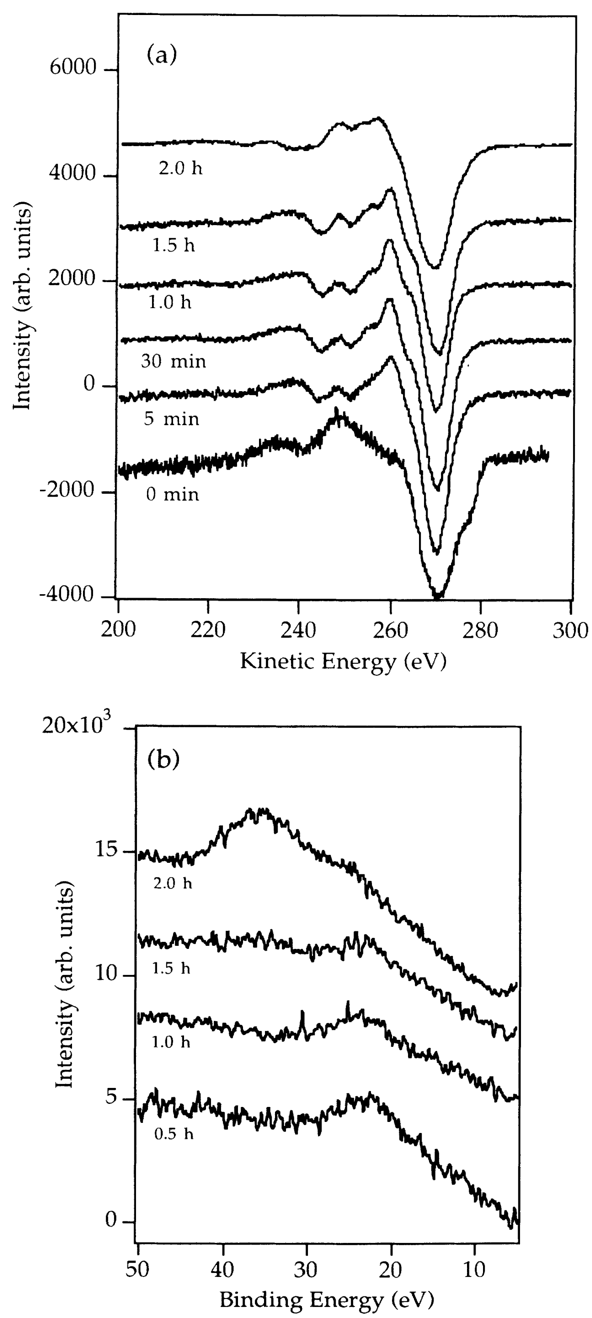

FIG. 7. Auger electron spectra and (b) XPS EELS taken at various bias times.

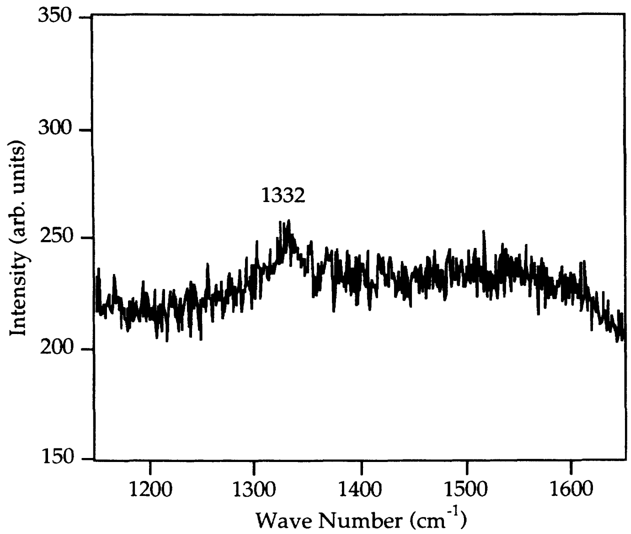

FIG. 8. Raman spectra from sample after 2 h of the bias pretreatment.

able nuclei present on the surface; thus it was difficult to obtain an accurate measure of the nucleation density. Therefore the nucleation density for the 30-min sample was determined based on a 30-min bias followed by a 10-h growth, which produced an approximately 75% complete diamond film. The density of particles on this sample was measured to be 1×10^7 cm^{-2}. Figure 10 shows a plot of resulting nucleation density as a function of bias time. The 0-min-bias sample is based on average values obtained from the literature for growth on untreated Si wafers. From these data it is evident that the nucleation density may be controlled over six orders of magnitude by varying the length of the bias pretreatment.

Data from AES, XPS EELS, Raman spectroscopy and SEM, obtained from the bias series, confirm that diamond is nucleating during the biasing pretreatment. Diamond particles may be observed by SEM at as early as 30 min of biasing. Nucleation continues for up to 2 h, at which time the surface is nearly covered with nuclei no larger that 80 nm in diameter. This confirms that the biasing process is actually creating the diamond nuclei, as opposed to just creating sites that are favorable for diamond nucleation. It is also important to note that if the bias pretreatment is allowed to continue long after the nominal 2-h limit, a much poorer-quality diamond film results, thus suggesting that conditions favorable for nucleation are not so for diamond growth.

In summary of the present section, the *in vacuo* surface-analytical series revealed several important stages in this diamond-nucleation process. First, there existed an amorphous nondiamond carbon on the surface before biasing began. This carbon layer was, within the first 5 min, either etched away or converted into Si-C as a thin Si-O layer was also formed. By 15 min of biasing, the Si-O layer was completely removed and the majority of the carbon on the surface was in the form of Si-C. From 5 min to 1 h of biasing, there existed a small surface layer of carbon, presumably on top of the Si-C. Overlayer calculations revealed that the carbide thickness reached a maximum of approximately 90 Å by 1 h of biasing and then decreased to near 50 Å by 2 h. The surface carbon was calculated to be approximately 5 Å thick at 5 min and increased to 10 Å by 1 h. XPS-EELS and Raman-

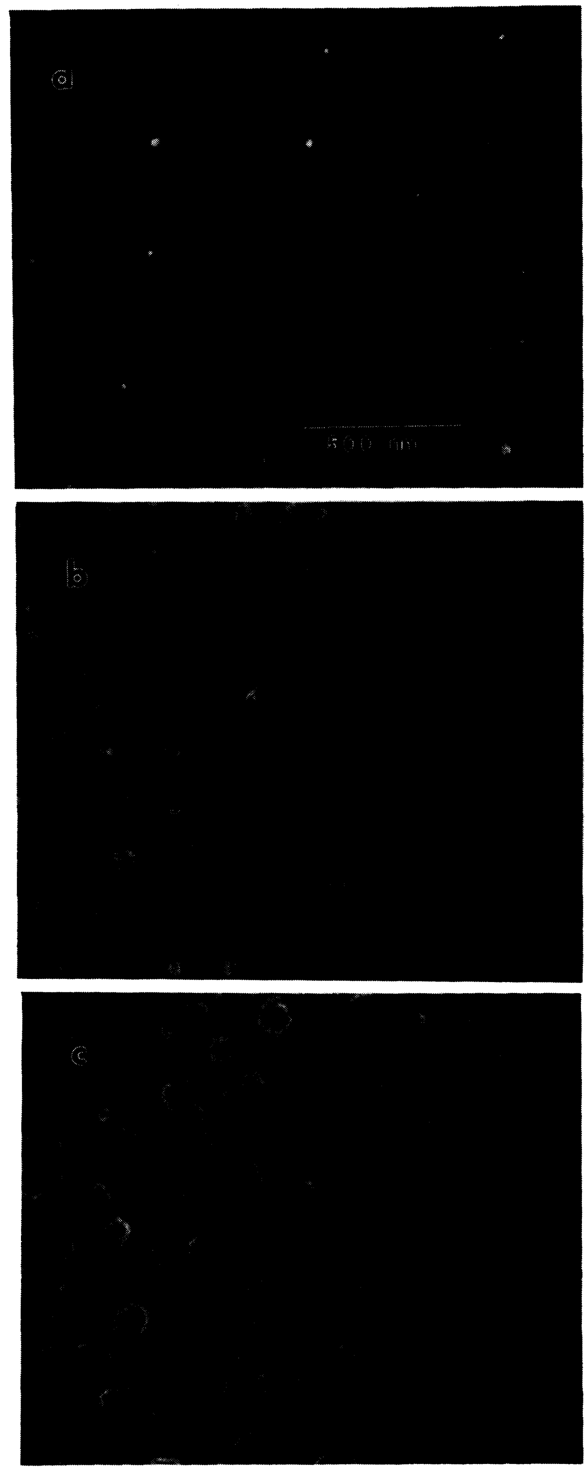

FIG. 9. SEM micrograph of the bias pretreatment after (a) 1.0 h, (b) 1.5 h, and (c) 2.0 h. Magnification scale is the same for all three.

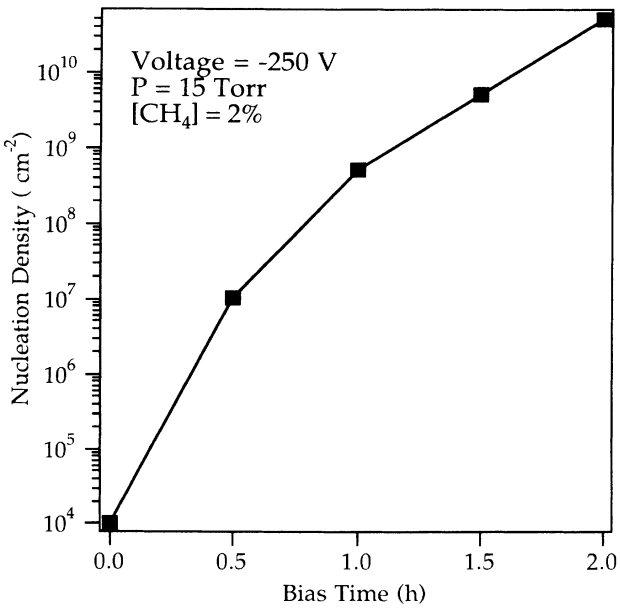

FIG. 10. Plot of nucleation density as a function of bias time. Nucleation density for 0.0-h-bias time taken from average literature values for growth on unscratched silicon.

spectroscopy data suggest that it is not graphitic and nucleation results exclude it from being diamond. It is believed that the Si-C is covered with a thin layer of amorphous carbon that has accumulated on the surface as a result of the biasing environment and that this carbon may play an important role in the nucleation of diamond during the bias-pretreatment process as discussed later.

C. Analytical series versus growth time (after a 1-h bias)

The data presented below were obtained by first biasing for 1 h and then intermittently performing surface analysis on the sample after periods of diamond growth with no biasing, as outlined in Sec. II. The diamond-growth times are defined as the period of time after the bias pretreatment has ended. The purpose of this series was to study the growth of diamond on the pretreated samples analyzed and discussed above. Table V displays the results from surface analysis for this series.

From observing the carbon 1*s* peak as a function of growth time [Fig. 11(a)], one notes a steady increase in C-C bonding (284.3 eV) from when the bias voltage is turned off and official growth begins, until the substrate is totally covered with diamond at the 5-h mark. Of special interest is the progression of the Si 2*p* peak [Fig. 11(b)]. When the bias is turned off at 1 h, the surface has been almost totally converted to SiC. After just 45 min of growth on this surface, the relative contribution of reduced Si to the total Si 2*p* peak has increased to 10%, while the carbon-to-silicon ratio has remained nearly con-

TABLE V. Quantification of species on the surface at various growth times for the 1-h-bias pretreatment, as calculated from XPS peak-area ratios.

Bias or growth time (h/h)	Carbon 1*s* peak ratios $I_{C\text{-}C}:I_{Si\text{-}C}$	Silicon 2*p* peak ratios $I_{Si\text{-}Si}:I_{Si\text{-}C}$ $(:I_{Si\text{-}O})$	Concentration ratios [C]/[Si]
0.0/0.0	$(C_xH_yO_z)$	100:0	16:84
0.08/0.0	22:78	44:43:(13)	26:74
0.25/0.0	22:78	26:74	32:68
0.5/0.0	20:80	20:80	33:67
1.0/0.0	20:80	1:99	37:63
1.0/0.75	43:57	10:90	35:65
1.0/1.0	50:50	14:86	41:59
1.0/2.0	76:24	35:65	52:48
1.0/5.0	100:0		100:0

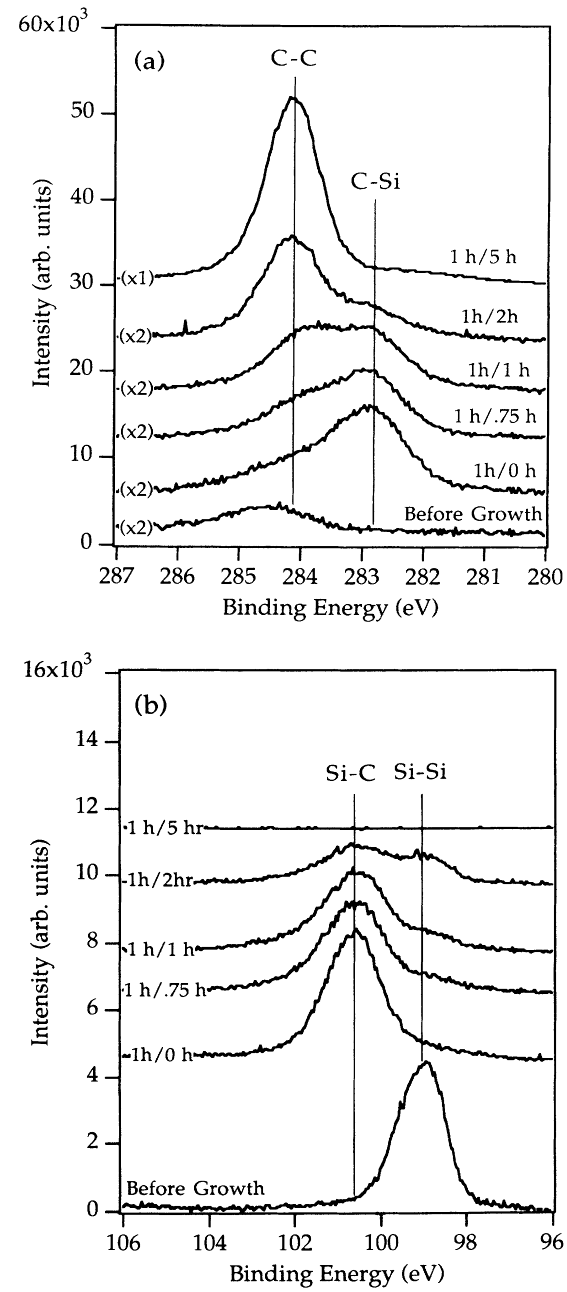

FIG. 11. XPS at various growth times after a 1-h-bias pretreatment: (a) carbon 1*s* and (b) silicon 2*p* peak progressions.

stant. This suggests that as the individual diamond particles are growing, as indicated by the increase in the C 1s peak at 284.3 eV, etching of the SiC surface or interfacial layer may be exposing silicon from the original substrate. It should be mentioned that it is not necessary to totally expose the silicon in order to observe it by XPS. Given the theoretical escape depth for Si, it should still be possible to observe the signal if it is covered by as much as 80–100 Å of SiC. If the SiC is amorphous, the escape depth may be slightly longer. After 2 h of growth following the biasing, the carbon-to-silicon ratio has increased to over 50%, with 76% of the C 1s signal originating from C-C bonding. The contribution from Si-Si bonding to the Si 2p peak has now increased to 35%, further suggesting that etching of the SiC interfacial layer may be continuing as the diamond particles continue to grow.

Overlayer calculations, similar to those performed for the previous series, indicate that once the bias is turned off, the silicon carbide layer begins to diminish rapidly. The interfacial layer reduces in average thickness, from 90 Å at the end of the biasing to 40 Å by 1 h and 20 Å by 2 h of growth. These data suggest again more convincingly that the silicon carbide layer is being etched, or removed, once significant diamond growth occurs. As mentioned in the previous section, the actual decrease in carbide thickness will not be as sharp if the etching, or removal of the carbide, is nonuniform.

As in the previous series, the AES spectra [Fig. 12(a)] continue to show a strong contribution from the SiC and do not resemble diamond until after 5 h of growth. The XPS-EELS series, on the other hand [Fig. 12(b)], shows that the contribution from diamond begins to become significant by 1.0 h of growth and continues until the film is complete at 5 h. Figure 13 displays SEM micrographs taken from sample (a) right after the 1-h bias and (b) after 1 h of growth. The micrographs show that after the bias is turned off, no more significant nucleation occurs and that the diamond growth continues primarily on the nuclei that existed at the end of the biasing period. The nucleation density remains roughly unchanged throughout the growth, and the average particle diameter increases in size.

It is important here to comment on the sensitivity of XPS EELS in observing diamond nucleation on, in this case, silicon carbide. Based on SEM data discussed above for the 1-h-biased sample (Fig. 13), the nucleation density of diamond particles on the surface was approximately 5×10^{8} cm^{-2} and they were 10–50 nm in diameter. This concentration may be too insignificant to be detected by XPS EELS. If one were to perform a rough area calculation based on an average particle diameter of 20 nm, the percentage of the sampling area covered by the diamond particles would be only 0.2%. For the sample that was grown for 1 h after biasing, the average particle diameter is near 100 nm. From this the average sampling area occupied by the diamond has increased to over 4%. Based on these calculations and the data presented above, the XPS core-level measurements are an effective means of determining the amount of specific phases on the surface during the nucleation process, but XPS EELS may only be used to obtain structural information for surface concentrations in excess of 2–4 %.

From the bias and growth series, the data suggest that diamond grows primarily on the diamond particles that existed on the surface after the initial biasing. SEM micrographs at different post-biasing growth times show that the initial particles just increase in size and develop better crystal habits with time. The discontinuation of nucleation once biasing ceases suggests again that ideal growth conditions may not be favorable for nucleation. As the diamond particles grow, there appears to be etch-

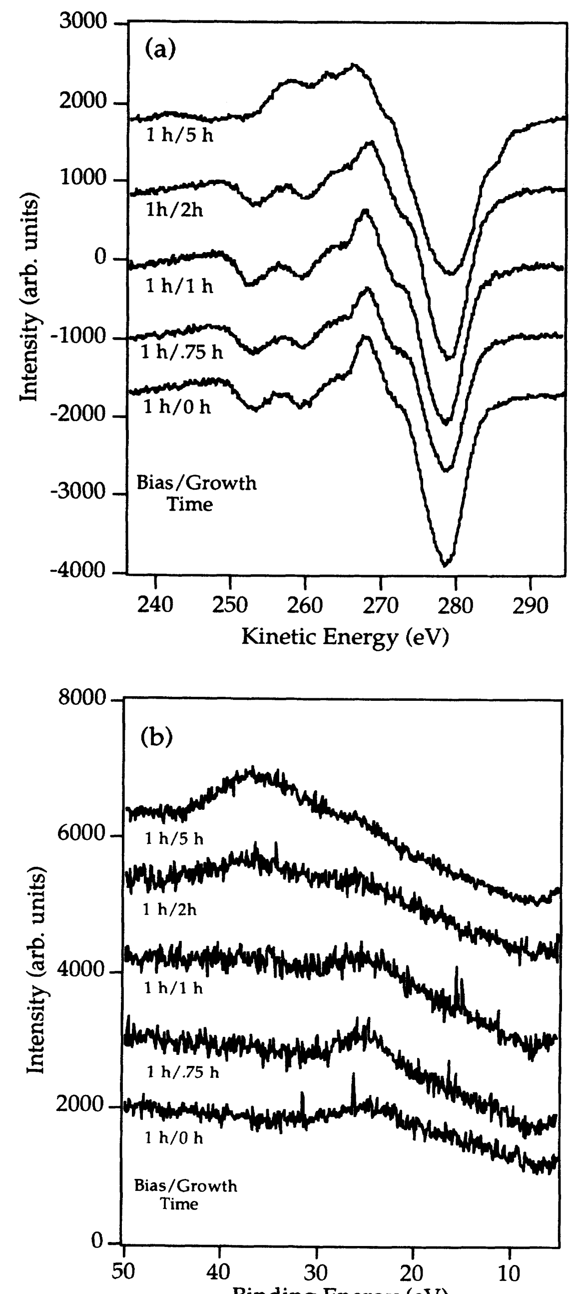

FIG. 12. (a) Auger electron spectra and (b) XPS EELS taken at various growth times on a sample bias pretreated for 1 h.

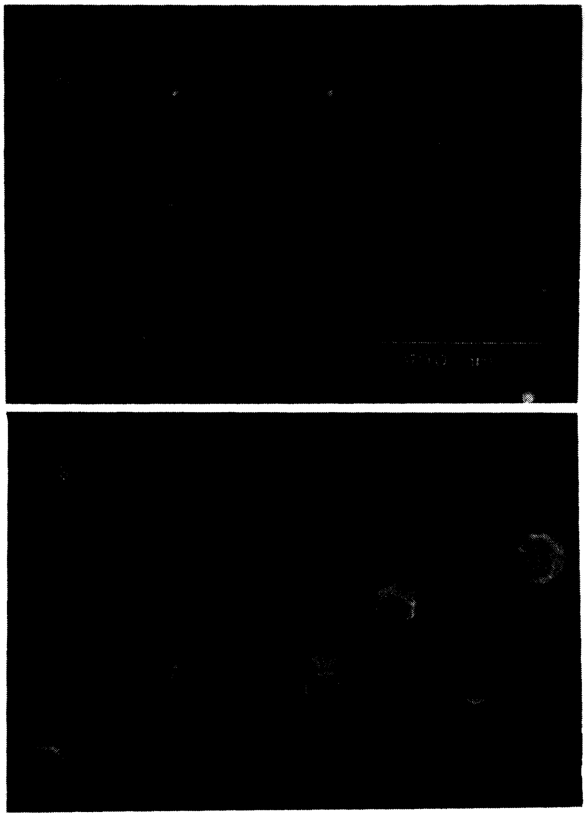

FIG. 13. SEM micrographs as a function of growth time on samples that were biased for 1 h, showing no new significant nucleation once the bias was turned off: (a) 1-h bias only and (b) 1-h growth after bias.

FIG. 14. Low-magnification high-resolution XTEM micrograph showing several nucleation sites and an interfacial layer between silicon and diamond.

ing of the SiC layer as suggested by the increase in the Si-Si bonding observed in the XPS Si $2p$ series.

D. Cross-sectional transmission electron microscopy

Figure 14 displays an XTEM micrograph from a sample that was biased for 1 h and then further grown for 5 h. The electron-beam direction was parallel to the Si$\langle 110 \rangle$ direction, such that the sample was viewed in an exact edge-on condition. An interfacial layer is readily observed between the silicon substrate and diamond film. Several diamond nuclei are seen to be emerging from this interfacial layer, and none were observed to be in direct contact with the Si substrate. This divergence of the initial nuclei reconfirms that CVD diamond undergoes three-dimensional growth once the stable nuclei has formed. Twin lamellae, prominent defects in diamond, were also observed just above where the nuclei begin to coalesce, as shown by the arrows in Fig. 14.

High-resolution TEM images were also obtained in the same region, as shown in Fig. 15. The grainy appearance of this interfacial layer under optimum focusing conditions revealed its noncrystalline, or amorphous, character. This was then confirmed by electron microdiffraction and optical diffractogramography. EELS was not performed in this region since its thickness was below the spatial resolution limit required for microanalysis in TEM. However, transmission EELS was performed on a separate sample that had a much thicker interfacial layer, and the spectra obtained were identical to a spectrum collected from single-crystal β-SiC under similar operating conditions. No other elements were found in these EELS spectra. Combined with the *in vacuo* surface analysis presented earlier, it is reasonable to assume that this interfacial layer is predominantly amorphous silicon carbide. The interfacial layer for the 1-h-bias sample appears to have an average thickness of approximately 60 Å, with some areas as thick as 100 Å.

It is important to determine whether the nuclei actually formed on top of this amorphous layer or on the surface of the silicon. Because the sample is viewed in cross section and because of the limited depth of field, the nuclei may only appear to have formed within the interfa-

FIG. 15. High-magnification high-resolution XTEM micrograph showing an amorphous interfacial layer between the diamond and silicon substrates.

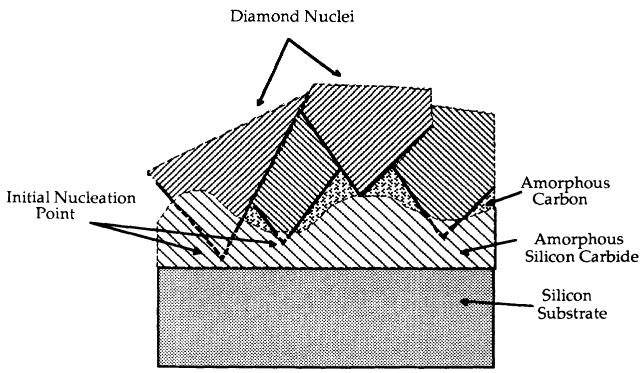

FIG. 16. Model of a diamond nuclei showing how nucleation may have occurred closer to the substrate than it appears.

cial layer, when, in fact, they may have formed on the silicon. If one models the nucleus as an inverted pyramid, it is easy to envision how a cross-sectional slice, not made in the exact center of the nucleus, can make it appear to have originated in the interfacial layer. However, by tracing the boundaries of the nuclei to a converging point, it appears that the nuclei originate within the interfacial layer and above the silicon substrate. This is shown schematically in Fig. 16 and may also be seen in Fig. 15. Furthermore, in all the samples examined, none of the diamond crystals were observed to be in direct contact with the Si substrate. Therefore it was concluded that nucleation did not occur on the silicon substrate directly, but rather on top of the interfacial layer.

IV. DISCUSSION

Based on the data presented above, as well as published studies on diamond nucleation, the authors have compiled a list of nucleation models or possible explanations for the enhancement of diamond nucleation resulting from a bias pretreatment. Since the emphasis of the present research involves this bias pretreatment, some nucleation mechanisms, although they may be valid under other experimental conditions, are not mentioned here. Listed below are four possible explanations for nucleation data presented in this study, and each will be discussed in greater detail in later sections: (a) diamond nucleation on adventitious carbon that existed on the surface before the biasing pretreatment, (b) diamond nucleation directly on an interfacial layer of either (i) crystalline silicon carbide or (ii) amorphous silicon carbide, (c) diamond nucleation on some stable nondiamond carbon that has accumulated on the surface during the biasing pretreatment, (d) diamond nucleation enhancement caused by the removal and suppression of a surface oxide.

A. Potential nucleation models

1. Nucleation on surface contamination present before biasing pretreatment

Williams,[30] in a study of the effect of various surface pretreatments on nucleation, has shown that a trend exists between the amount of carbon observed on the surface before growth and the resulting nucleation density. Samples that had higher amounts of carbon on the surface resulted, qualitatively, in higher nucleation densities. One possible source of nucleation enhancement could have been from the adventitious carbon found on the substrate prior to biasing. However, a problem with this model is that similar concentrations of adventitious carbon were found on the surfaces of unscratched silicon wafers in Williams's study and the resulting nucleation densities were very low. One might then argue that, during the biasing, this carbon is converted into a form suitable for nucleation. From the surface-analytical series versus bias time discussed in Sec. III B, it was found that within the first 5 min of biasing the adventitious carbon had either been replaced by or converted into a mixture of C-C and Si-C. If the conversion of the adventitious carbon, via biasing, is the explanation for increased nucleation, then one would expect a significantly higher nucleation density after just 5 min of biasing. This suggests that the surface contamination alone does not account for the observed increase in nucleation density.

2. Nucleation directly on silicon carbide

Silicon carbide was observed in this study to have formed on the silicon surface before the diamond particles could be detected. Both Belton *et al.*[36] and Williams *et al.*,[38] in similar *in vacuo* studies, also observed the formation of Si-C during the early stages of diamond growth. Polycrystalline silicon carbide has also been observed by many other researchers[32–35,59] to have formed between the diamond and silicon substrate. Badzian and Badzian[60] have suggested that the development of a β-SiC buffer layer is first required before diamond nucleates on silicon. These arguments were made based on a partial lattice matching observed on the (110) when the $\langle 100 \rangle$ direction of β-SiC is parallel to the $\langle 112 \rangle$ direction of diamond. Hartnett *et al.*[41] reported 3 times higher diamond-nucleation densities on (220)-textured CVD-grown β-SiC films than on untreated silicon, but no enhancement for growth on ion-sputtered SiC and (111)-textured β-SiC films.

The authors believe that the formation of silicon carbide plays a role in diamond nucleation on silicon, but that it is not alone sufficient for nucleation to occur. The focus of this discussion should not be on whether diamond can be grown on a SiC substrate or whether an interfacial SiC layer forms before diamond growth on silicon, but rather on the actual steps by which diamond forms on the SiC. Does the nucleation occur directly on the silicon carbide, or is there another intermediate step that must occur?

One of the first problems with the hypothesis that diamond nucleation occurs directly on SiC is the relatively small increase in nucleation density observed when SiC substrates are used. The reports show as much as 3 times higher nucleation density on SiC substrates,[41] but the biasing pretreatment used in this study increased nucleation by several orders of magnitude beyond that. Furthermore, if the presence of silicon carbide is the sole requirement for nucleation to occur, then one would expect much higher nucleation densities for the shorter bias times since a SiC layer forms immediately. It could be argued that it is the amorphous character of the SiC layer in the present research that promotes higher nucleation rates. An amorphous surface has a higher surface free energy, and it is thus more energetically favorable for nucleation to occur on such a surface. However, this alone cannot explain the large change observed in nucleation density as a function of bias time since this amorphous layer essentially forms immediately. Furthermore, as mentioned previously, on sputtered SiC no significant increase in nucleation was observed.[41]

Another problem with the theory that diamond nucleates directly on the carbide is expressed in reports of nucleation-enhancement techniques that do not involve carbide formation. Angus *et al.* have achieved high nucleation densities by sprinkling graphite powder on the substrate surface,[45] while Morrish *et al.*[23,24] were equally successful with pump oil as a nucleation promoter. Furthermore, one of the present authors has also observed in a separate study[61] that under some conditions amorphous carbon interfacial layers exist between the diamond film and silicon substrate rather than a SiC layer. Finally, scratching a Si substrate is not expected to modify the formation of SiC significantly, yet it has a major impact on nucleation density.

These data suggest that some type of a carbonaceous precursor may be involved and that the carbide formation only plays an intermediate role. Recall that the XPS data for the bias series (Table III and Fig. 5) showed that from 5 min to 1 h of biasing there existed an excess concentration of elemental carbon on the SiC surface. This excess carbon again suggests that the nucleation of diamond directly on silicon carbide may not be the primary explanation for the increased density from biasing and is the topic of the next section (Sec. IV A 3).

3. *Nucleation of a non-diamond carbonaceous precursor*

The majority of the data from the literature as well as from this study suggest that some intermediate nucleation step exists between the carbide formation and actual diamond nucleation. In the data presented here, amorphous silicon carbide was immediately formed (1–5 min) on the surface of the silicon. There also existed a small amount of amorphous carbon (it was determined to be neither graphite nor diamond) on the surface of the Si-C. This "excess" carbon may have resulted from (1) increased flux of positively charged carbon and hydrocarbon ions to the surface or (2) nonuniform etching or sublimation of the silicon carbide. Van Bommel, Crombeen, and Tooren,[52] found that silicon could preferentially evaporate from SiC thus leaving the surface carbon rich. In the present work, as the carbide layer continues to grow from 5 min to 1 h, the concentration of this amorphous layer relative to the carbide remains fairly constant. After 1 h of bias the amorphous carbon can no longer be distinguished from the diamond nuclei on the surface using XPS core-level shifts. It is hypothesized that this surface carbon contributes significantly to the nucleation of diamond and that the silicon carbide merely acts as a temporary but critical host on which the carbon can accumulate until clusters of the appropriate size and structure required for diamond nucleation develop.

Before attacking the specific problem of diamond nucleation, one should first consider the basic steps involved in the nucleation of three-dimensional clusters. General cluster-nucleation phenomena may be simplified and explained as a series of the following steps.[62]

(i) Atoms impinge upon the substrate from the vapor phase and become adsorbed onto the surface.

(ii) At standard CVD temperatures, the adatoms, if they are not free to react with the substrate, may either reevaporate or diffuse over the surface.

(iii) If the concentration of adatoms is high enough, they combine and form clusters.

(iv) Through statistical fluctuations in local adatom concentration, these clusters grow and decay.

(v) Because of free-energy considerations, there will be a critical size above which the probability of growth will be greater than decay.

(vi) These stable clusters are then free to grow either from the continued migration of single adatoms or from the direct impingement of atoms from the vapor phase.

In the cases of bias-enhanced diamond nucleation, the proposed model is only slightly more complicated in that it first involves the formation of an interfacial carbide layer. When the carbon first arrives at the surface, it is more energetically favorable to form silicon carbide than for the atoms to accumulate on the surface and eventually form clusters. Silicon carbide formation, however, is kinetically limited by silicon diffusion through the existing carbide layer to the surface. Thus, although there initially exists an excess concentration of carbon on the surface, it may not be kinetically favorable for critical nuclei to form until after the carbide has reached a critical thickness such that the silicon outdiffusion is too slow to continue. However, in contradiction to this argument, data show that the carbide layer is still growing from 30 to 60 min, yet nucleation has occurred as early as 30 min and is easily visible by 1 h. The reason for this is believed to be that local islands of Si-C have reached a critical thickness such that the carbon on the surface is then allowed to cluster and eventually form a stable, suitable site for diamond nucleation. This also helps explain the rapid increase in nucleation as a function of bias time. As more and more areas reach critical carbide thicknesses, more carbon becomes available to form stable clusters. This variation in thickness of the interfacial SiC layer is supported by the TEM observations.

TEM observations also show that nucleation is occurring closer to the Si/SiC interface than the critical thickness described above. One possible explanation for this may be due to the etching of the SiC. If during the etching process silicon is being preferentially depleted, excess carbon could locally saturate the surface. This local saturation of carbon would allow critical carbon clusters, and eventually diamond nuclei, to form in a region where the carbide is below the critical thickness.

It is important to stress that, although the carbon clusters on the surface may reach a critical size, they may not be ideally suited for diamond nucleation. Reports have shown that amorphous carbon alone does not act as a strong nucleation promoter.[22,41] The authors suggest that certain clusters may form that, at least locally or in certain regions, have the correct crystal structure and bonding configuration to promote the formation of the diamond structure. This speculation is based on the observations that not all forms of carbon are sufficient for diamond nucleation. Unfortunately, the exact form of this excess carbon necessary for diamond growth is not known, although Angus[47] has recently made some progress in this area, utilizing graphite as the starting point for his model. Judging from the much higher nucleation densities achieved on carbide-versus non-carbide-forming substrates, either the amount or type of excess carbon present is related to the carbide-forming properties of the substrate. There are numerous mechanisms which may account for this influence, including the items discussed in the following sections.

B. Role of biasing in enhancing the nucleation

The previous section provided suggestions for nucleation models and the critical steps that may lead up to nucleation. The role that biasing plays in either promoting or accelerating these critical steps is of interest as well. Does the biasing merely accelerate the same process that would otherwise occur at much slower rates, or does it create alternative path(s) that would not occur, under standard CVD conditions? The following are the envisioned possible effects that biasing may have on the CVD process in so far as they relate to diamond nucleation: (i) increased flux of positively charged carbon ions to the surface ($C_xH_y{}^+$); (ii) reduced flux of electrons and negatively charged ions to the surface; (iii) higher-energy transfer from the ions to the surface, resulting in increased surface mobilities of adsorbed species; (iv) enhancement of reactions and molecular dissociation just above the substrate as a result of an increase in, and higher energy for, ion-neutral collisions within the sheath region; and (v) reduction and suppression of oxide formation on the surface.

It is easy to conceptualize how an increase in the arrival rate of carbon or hydrocarbon ions to the surface may help to expedite the nucleation process as outlined above. The possible role of electrons in preventing or suppressing nucleation is unclear. Since electrons are being repelled during the negative biasing, one may suggest that they may indeed inhibit nucleation. However, positive biasing during hot-filament CVD experiments did not significantly suppress diamond nucleation.[63,64]

The approximate ion-impingement energy may be calculated from the Stefan-Boltzmann law,

$$E=\sigma T^4 ,$$

by measuring the increase in temperature as a result of the biasing. From this relationship the ion energies were calculated to be approximately 5 eV. Ions of this energy are not expected to create much damage to the surface, although some energy is expected to be transferred upon collision with substrate atoms. Ion bombardment of the surface could locally increase the surface mobilities of adatoms and may thus help to explain how carbon clusters can form more rapidly on the surface. It may also explain why the interfacial layer is amorphous. The continual ion bombardment may prevent the amorphous-surface carbide from crystallizing.

The increased dissociation due to accelerated ions in the sheath region is easy to envision, yet again the consequences are unclear. The ions that are accelerated through the sheath region have a much higher kinetic energy than in the rest of the plasma; therefore, when they collide with another ion or neutral molecule, there is a higher ionization or dissociation efficiency. This could result in a much higher concentration of dissociated hydrocarbons, and atomic hydrogen, near the sample surface.

Since oxide formation does play a significant role in inhibiting diamond nucleation, it is necessary to discuss the role that the elimination of oxide formation might play during bias-enhanced nucleation. It is agreed by most researchers that the presence of a native oxide on silicon will impede the nucleation process. SiO_2 masks have been used widely as a method of obtaining selected-area nucleation of diamond.[65,66] On a similar *in vacuo* study performed by Williams *et al.*[38] on a silicon substrate prepared by scratching only, Si-O was observed throughout the entire analytical series. The present study was performed using the same *in vacuo* growth and analytical chamber. The current data from the biasing series showed that no Si-O could be detected after 15 min indicating that the biasing is very effective in removing the oxide.

The actual mechanism by which the oxide is removed is unclear; however, initial results in the authors' laboratory showed that biasing in a hydrogen plasma alone were unsuccessful in removing the oxide. This preliminary data suggest that a reaction involving the C-O bond is responsible for the removal of Si-O. Lee, Miller, and Cutler[67] proposed the following mechanism by which SiO_2 may be reduced by carbon:

$$SiO_2+CO \rightarrow SiO+CO_2 , \tag{1}$$

$$C+CO_2 \rightarrow 2CO , \tag{2}$$

$$SiO+2C \rightarrow SiC+CO . \tag{3}$$

Once the reaction is initiated, CO will be regenerated as long as there is SiO_2 available. The initial CO gas required to initiate the above reaction may be obtained from the solid-solid reaction between initial carbon species arriving on the surface and the oxide according to the reaction

$$SiO_2+3C \rightarrow SiC+2CO . \tag{4}$$

Reaction (4) has also been suggested by Pickrell *et al.*[68] as an intermediate reaction for the nucleation of diamond on silica. An increase in the flux and kinetic energy of $C_xH_y{}^+$ species to the surface may help explain why the oxide becomes less stable under biasing conditions. If the arriving carbon species have higher kinetic energy as a result of the biasing, then reactions (2)–(4) may proceed more rapidly to the right, thus resulting in an increased removal of oxide from the surface. The authors are not suggesting that the elimination of the oxide alone should explain the substantial increase in nucleation density; however, it should be considered as to have played a major role in allowing nucleation to occur. Once the oxide has been eliminated, the other major nucleation steps, as outlined in the previous section, must then occur for the successful development of the diamond nuclei.

The above are only speculations on how the biasing may be aiding the nucleation process. A more in-depth discussion requires a much greater understanding and more thorough study of the plasma conditions during this biasing process. Plasma diagnostics within the sheath region, under various biasing conditions, would be very beneficial in aiding the understanding of bias-enhanced diamond nucleation.

C. Schematic summary of the nucleation model

In view of the previous discussions, a schematic representation of the steps for nucleation which are speculated to be important can be developed. This is displayed in Fig. 17.

(i) Before biasing begins there are both adsorbed oxygen and amorphous carbon present on the silicon surface [Fig. 17(a)].

(ii) The adsorbed carbon is then either etched away or converted to Si-C, and the physisorbed oxygen is converted into Si-O [Fig. 17(b)].

(iii) As biasing continues, the oxide is etched as the carbide islands continue to grow. Preferential etching of the silicon from the Si-C and/or continued high flux of carbon to the surface creates an excess concentration of carbon on the surface [Fig. 17(c)].

(iv) As the local carbide islands reach a critical thickness, such that continued carbide growth is unlikely, the excess carbon on the surface becomes free to form small clusters. Surface mobility of the carbon may be enhanced by the bombardment during the biasing.

(v) Some of these clusters become favorable for diamond nucleation [Fig. 17(d)].

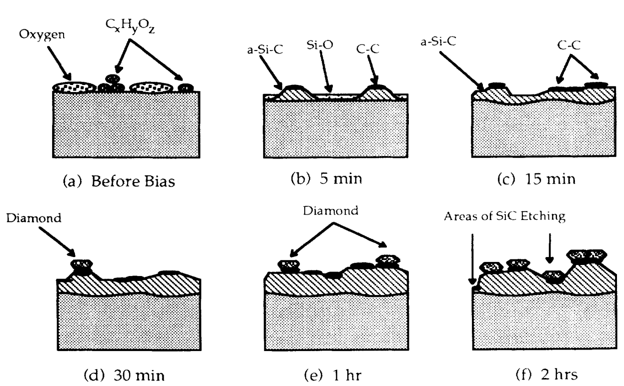

FIG. 17. Model of diamond nucleation, via biasing, on silicon.

(vi) As most of the carbide reaches a critical thickness (90 Å), more free carbon becomes available to form other diamond-nucleation sites, and thus a greater number of diamond nuclei are observed [Fig. 17(e)].

(vii) As biasing continues, there is ongoing etching of the surface (but not the more stable diamond nuclei) and adsorption of the carbon. This local etching creates a rougher silicon carbide surface. If silicon is preferentially etched from the carbide, increasing the carbon concentration in that region, then nucleation clusters may actually form on thinner areas of the carbide.

(viii) The etching, cluster formation, and diamond nucleation continue until the surface is eventually covered with diamond nuclei [Fig. 17(f)].

V. SUMMARY

It has been shown here that biasing may be used as an effective means of nucleation enhancement. The major purpose of this work was to gain a better understanding of this method of enhancing diamond nucleation on silicon. *In vacuo* surface analysis as well as high-resolution XTEM, SEM, and Raman spectroscopy were used to study the nucleation and growth of diamond using-biasing and microwave plasma CVD. Biasing was found to increase the nucleation density for unscratched silicon substrates by over five orders of magnitude. The nucleation density may be controlled over three orders of magnitude by varying the length of the bias pretreatment. Once the bias was turned off, diamond grew on diamond nuclei that were created during the pretreatment and no further significant nucleation occurred. If the bias was left on indefinitely, the resulting diamond film was of much poorer quality than that produced under a 1–2-h bias followed by a growth with no bias. This suggested that conditions which are favorable for diamond nucleation are not ideal for diamond growth.

An amorphous silicon carbide interfacial layer developed before significant diamond nucleation occurred. Preferential etching of the Si-C and/or a decreased reaction with Si were thought to be responsible for the development of an excess carbon concentration on the Si-C. Once the silicon carbide layer had reached a critical or maximum thickness, which under these experimental conditions was approximately 90 Å, it was believed that the carbon on the surface was free to form critical clusters that were eventually favorable for diamond nucleation. Once significant diamond nucleation has occurred, the preferential etching of the carbide appears to have allowed carbon clusters to form on thinner regions, closer to the Si substrate, thus explaining why some diamond nuclei were observed to be closer to the substrate than others. The ability of the biasing pretreatment to remove and suppress the formation of a surface oxide was also thought to play a role in the nucleation enhancement.

ACKNOWLEDGMENTS

The authors wish to thank X. H. Wang and R. J. Nemanich for performing the Raman spectroscopy and M. Veil for assisting with the diamond growth. Technical assistance from K. L. More and N. D. Evans in performing HRTEM and EELS analysis at Oak Ridge National Laboratory is also deeply appreciated. Useful advice from D. Belton and J. Angus is also gratefully acknowledged. This research was financially supported in part by SDIO/IST through ONR and by Kobe Steel, Ltd. Transmission EELS analysis was supported in part by the Division of Materials Sciences, U.S. Department of Energy through the SHaRE Program under Contract No. DE-AC05-76OR00033 with Oak Ridge Associated Universities. High-resolution TEM was sponsored by the U.S. Department of Energy, Office of Transportation Technologies, as part of the High Temperature Materials Laboratory User Program, under Contract No. DE-AC05-84OR21400 with Martin Marietta Energy Systems, Inc.

[1]S. Matsumoto, Y. Sato, M. Kamo, and N. Setaka, Jpn. J. Appl. Phys. **21**, L183 (1982).

[2]D. V. Fedoseev, B. V. Deryagin, I. G. Varshavskaya, A. V. Lavrent'ev, and V. V. Matveev, Zh. Eksp. Teor. Fiz. **80**, 413 (1981) [Sov. Phys.—JETP **53**, 210 (1981)].

[3]R. Mania, L. Stobierski, and R. Pampuch, Cryst. Res. Technol. **16**, 785 (1981).

[4]S. Matsumoto, Y. Sato, M. Tsutsumi, and N. Setaka, J. Mater. Sci. **17**, 3106 (1982).

[5]D. V. Fedoseev, Kolloidn. Zh. [Colloid J. USSR **46**, 727 (1984)].

[6]D. V. Fedoseev, I. G. Varshavskaya, and B. V. Derjaguin, J. Electrochem. Soc. **81**, 284 (1981).

[7]D. V. Fedoseev and T. S. A. S. Semenova, Sov. J. Superhard Mater. **6**, 1 (1984).

[8]M. Frenklach, W. Howard, D. Huang, J. Yuan, K. E. Spear, and R. Koda, Appl. Phys. Lett. **59**, 546 (1991).

[9]M. Frenklach, R. Kematic, D. Huang, W. Howard, K. E. Spear, A. W. Phelps, and R. Koba, J. Appl. Phys. **66**, 395 (1989).

[10]J. C. Angus, H. A. Will, and W. S. Stanko, J. Appl. Phys. **39**, 2915 (1968).

[11]W. Howard, D. Huang, J. Yuan, M. Frenklach, K. E. Spear, R. Koba, and A. W. Phelps, J. Appl. Phys. **68**, 1247 (1990).

[12]S. Mitura, J. Cryst. Growth **80**, 417 (1987).

[13]P. K. Bachmann, W. Drawl, D. Knight, R. Weimer, and R. F. Messier, in *Diamond and Diamond-Like Materials Synthesis,* edited by G. H. Johnson, A. R. Badzian, and M. W. Geis (Materials Research Society, Pittsburgh, 1988), p. 99.

[14]P. K. Bachmann, R. Weimer, W. Drawl, Y. Liou, and R. Messier (unpublished).

[15]S. Iijima, Y. Aikawa, and K. Baba, Appl. Phys. Lett. **57**, 2646 (1990).

[16]S. Iijima, Y. Aikawa, and K. Baba, J. Mater. Res. **6**, 1491 (1991).

[17]K. Suzuki, A. Sawabe, H. Yasuda, and T. Inuzaka, Appl. Phys. Lett. **50**, 728 (1987).

[18]A. Sawabe and T. Inuzuka, Thin Solid Films **137**, 89 (1986).

[19]C.-P. Chang, D. L. Flamm, D. E. Ibbotson, and J. A. Mucha, J. Appl. Phys. **63**, 1744 (1988).

[20]K. V. Ravi and C. A. Koch, Appl. Phys. Lett. **57**, 348 (1990).

[21]K. V. Ravi, C. A. Koch, H. S. Hu, and A. Joshi, J. Mater. Res. **5**, 2356 (1990).

[22]J. J. Dubray, C. G. Pantano, M. Meloncelli, and E. Bertran, J. Vac. Sci. Technol. A **9**, 3012 (1991).

[23]A. A. Morrish, K. Snail, and W. Carrington (unpublished).

[24]A. A. Morrish and P. E. Pehrsson, Appl. Phys. Lett. **59**, 417 (1991).

[25]B. R. Stoner, B. E. Williams, S. D. Wolter, K. Nishimura, and J. T. Glass, J. Mater. Res. **7**, 257 (1992).

[26]S. Yugo, T. Kanai, T. Kimura, and T. Muto, Appl. Phys. Lett. **58**, 1036 (1991).

[27]P. A. Dennig and D. A. Stevenson, in *Proceedings of the Second International Conference on the New Diamond Science and Technology,* edited by R. Messier and J. T. Glass (Japan New Diamond Forum, Washington, D.C., 1990).

[28]P. A. Dennig and D. A. Stevenson, in *Proceedings of the First International Conference on the Applications of Diamond Films and Related Materials,* edited by Y. Tzeng, M. Yoshikawa, M. Murakawa, and A. Feldman (Elsevier, New York, 1991), p. 383.

[29]A. R. Kirkpatrick, B. W. Ward, and N. P. Economou, J. Vac. Sci. Technol. B **7**, 1947 (1989).

[30]B. E. Williams (unpublished).

[31]D. E. Meyer, R. O. Dillon, and J. A. Woollam, J. Vac. Sci. Technol. A **7**, 2325 (1989).

[32]S. Yugo, T. Kimura, and T. Muto, Vacuum **41**, 1364 (1990).

[33]S. Yugo, T. Kimura, H. Kanai, and Y. Adachi, in *Noble Refractory Semiconductors,* edited by D. Emin, T. Aselage, and C. Wood, MRS Symp. Proc. No. 97 (Materials Research Society, Pittsburgh, 1987), p. 327.

[34]B. E. Williams, D. A. Asbury, and J. T. Glass, in *Surface Analysis of Diamond Nucleation on Silicon and Electron Microscopy of the Diamond/Silicon Interface,* edited by R. Freer (Kluwer Academic, Amsterdam, 1990), p. 169.

[35]B. E. Williams and J. T. Glass, J. Mater. Res. **4**, 373 (1989).

[36]D. N. Belton, S. J. Harris, S. J. Schmieg, A. M. Wiener, and T. A. Perry, Appl. Phys. Lett. **54**, 416 (1989).

[37]D. N. Belton and S. J. Schmieg, J. Vac. Sci. Technol. A **8**, 2353 (1990).

[38]B. E. Williams, B. R. Stoner, D. A. Asbury, and J. T. Glass, in *Diamond and Diamond-Like Films and Coatings, NATO Advanced Study Institute, Series B: Physics,* edited by J. Angus, R. Clausing, L. Horton, and P. Koidl (Plenum, New York, 1990).

[39]P. O. Joffreau, R. Haubner, and B. Lux (unpublished).

[40]P. O. Joffreau, R. Haubner, and B. Lux, Int. J. Refract. Hard Met. December, 186 (1988).

[41]T. Hartnett, R. Miller, D. Montanari, C. Willingham, and R. Tustison, J. Vac. Sci. Technol. A **8**, 2129 (1990).

[42]D. N. Belton and S. J. Schmieg, J. Appl. Phys. (to be published).

[43]S. J. Harris, D. N. Belton, A. M. Weiner, and S. J. Schmieg, J. Appl. Phys. **66**, 5353 (1989).

[44]D. N. Belton and S. J. Schmieg, J. Appl. Phys. **66**, 4223 (1989).

[45]J. C. Angus, Z. Li, M. Sunkara, R. Gat, A. B. Anderson, S. P. Mehandru, and M. W. Geis, in *Proceedings of the International Symposium on Diamond and Diamond Materials, Electrochemical Society Meeting, Washington, D.C.* (Electrochemical Society, New York, in press).

[46]R. A. Rudder, G. C. Hudson, R. C. Hendry, R. E. Thomas, J. B. Posthill, and R. J. Markunas, in *Proceedings of the First In-*

ternational Conference on the Applications of Diamond Films and Related Materials, edited by Y. Tzeng, M. Yoshikawa, M. Murakawa, and A. Feldman (Elsevier, New York, 1991), p. 395.
[47]J. C. Angus (unpublished).
[48]G.-H. M. Ma, Y. H. Lee, and J. T. Glass, J. Mater. Res. **5**, 2367 (1990).
[49]G.-H. M. Ma, B. E. Williams, J. T. Prater, and J. T. Glass, Diamond Relat. Mater. **1**, 25 (1991).
[50]R. E. Shroder, R. J. Nemanich, and J. T. Glass, Phys. Rev. B **41**, 3738 (1990).
[51]R. J. Nemanich, J. T. Glass, G. Lucovsky, and R. E. Shroder, J. Vac. Sci. Technol. A **6**, 1783 (1988).
[52]A. J. Van Bommel, J. E. Crombeen, and A. V. Tooren, Surf. Sci. **48**, 463 (1975).
[53]M. P. Seah and W. A. Danch, Surf. Interface Anal. **1**, 2 (1979).
[54]C. S. Fadley, R. J. Baird, W. Siekhaus, T. Novakov, and S. A. L. Bergstrom, J. Electron Spectrosc. Relat. Phenom. **4**, 93 (1974).
[55]L. C. Feldman and J. W. Mayer, *Fundamentals of Surface and Thin Film Analysis* (Elsevier, New York, 1986).
[56]Y. Wang, R. W. Hoffman, and J. C. Angus, J. Vac. Sci. Technol. A **8**, 2226 (1990).
[57]Y. Wang, H. Chen, R. W. Hoffman, and J. C. Angus, J. Mater. Res. **5**, 1 (1990).
[58]J. T. Glass, B. E. Williams, and R. F. Davis, Proc. Soc. Photo-Opt. Instrum. Eng. **877**, 56 (1988).
[59]Y. Mitsuda, Y. Kojima, T. Yoshida, and K. Akashi, J. Mater. Sci. **22**, 1557 (1987).
[60]A. R. Badzian and T. Badzian, Surf. Coat. Technol. **36**, 283 (1988).
[61]G.-H. M. Ma, Ph.D. dissertation, North Carolina State University, 1991.
[62]J. L. Robins, Appl. Surf. Sci. **33/34**, 379 (1988).
[63]Y.-H. Lee, Ph.D. dissertation, North Carolina State University, 1990.
[64]Y. H. Lee, P. D. Richard, K. J. Bachmann, and J. T. Glass, Appl. Phys. Lett. **56**, 620 (1990).
[65]J. L. Davidson, C. Ellis, and R. Ramesham, J. Electron. Mater. **18**, 711 (1989).
[66]J. Ma, H. Kawarada, T. Yonehara, J.-I. Suzuki, J. Wei, Y. Yokota, and A. Hiraki, Appl. Phys. Lett. **55**, 1071 (1989).
[67]J. G. Lee, P. D. Miller, and I. B. Cutler, in *Proceedings of the Eighth International Symposium on the Reactivity of Solids,* edited by J. Wood, O. Lindqvist, C. Helgesson, and N.-G. Vannerberg (Plenum, New York, 1977), p. 707.
[68]D. J. Pickrell, W. Zhu, A. R. Badzian, R. E. Newnham, and R. Messier, J. Mater. Res. **6**, 1264 (1991).

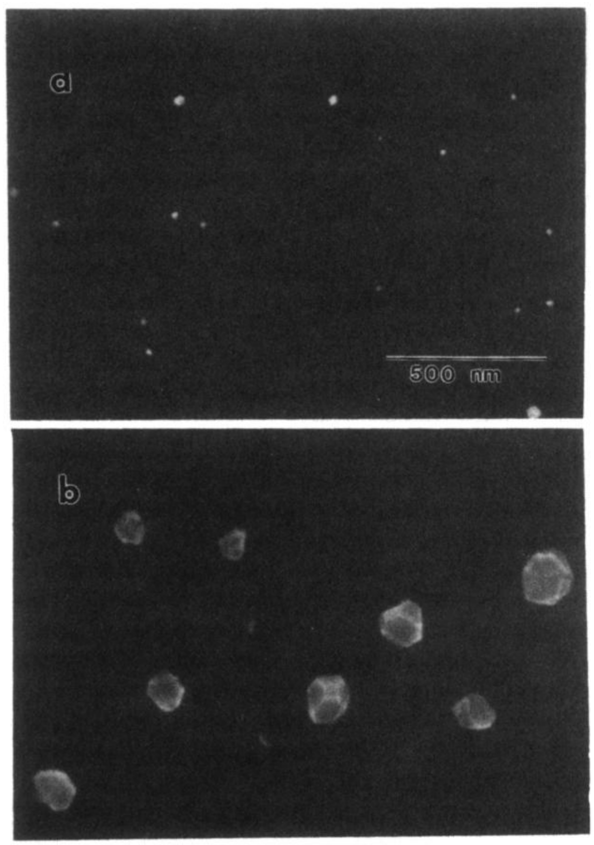

FIG. 13. SEM micrographs as a function of growth time on samples that were biased for 1 h, showing no new significant nucleation once the bias was turned off: (a) 1-h bias only and (b) 1-h growth after bias.

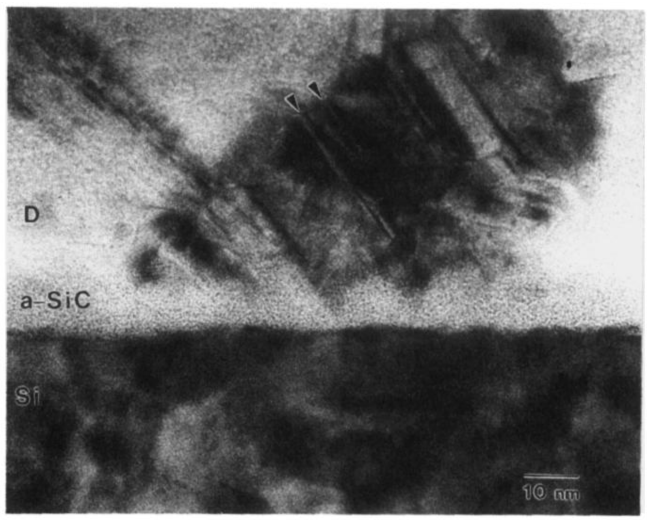

FIG. 14. Low-magnification high-resolution XTEM micrograph showing several nucleation sites and an interfacial layer between silicon and diamond.

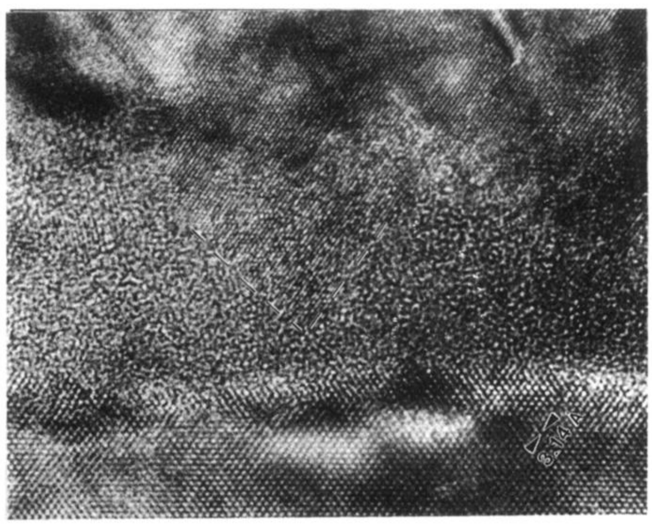

FIG. 15. High-magnification high-resolution XTEM micrograph showing an amorphous interfacial layer between the diamond and silicon substrates.

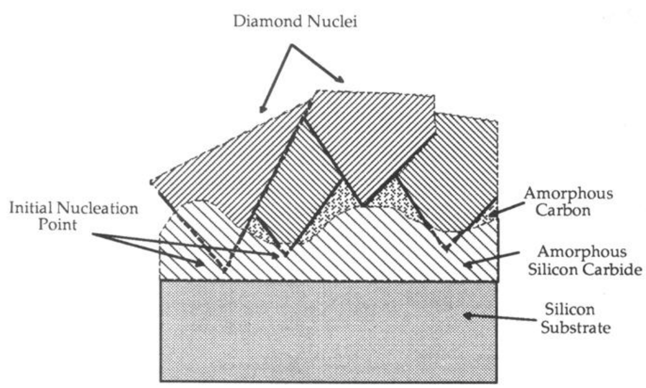

FIG. 16. Model of a diamond nuclei showing how nucleation may have occurred closer to the substrate than it appears.

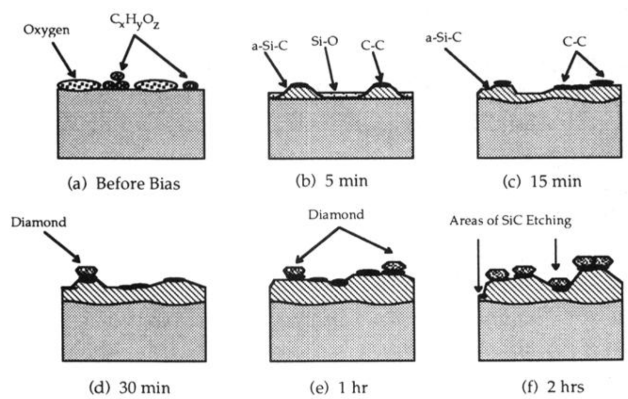

FIG. 17. Model of diamond nucleation, via biasing, on silicon.

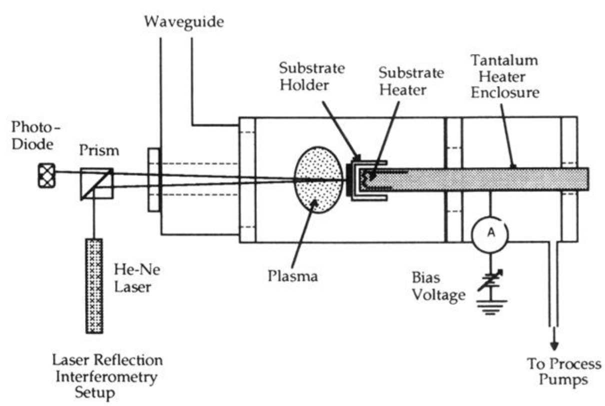

FIG. 2. CVD chamber showing *in situ* laser-reflection interferometry and substrate-biasing arrangements.

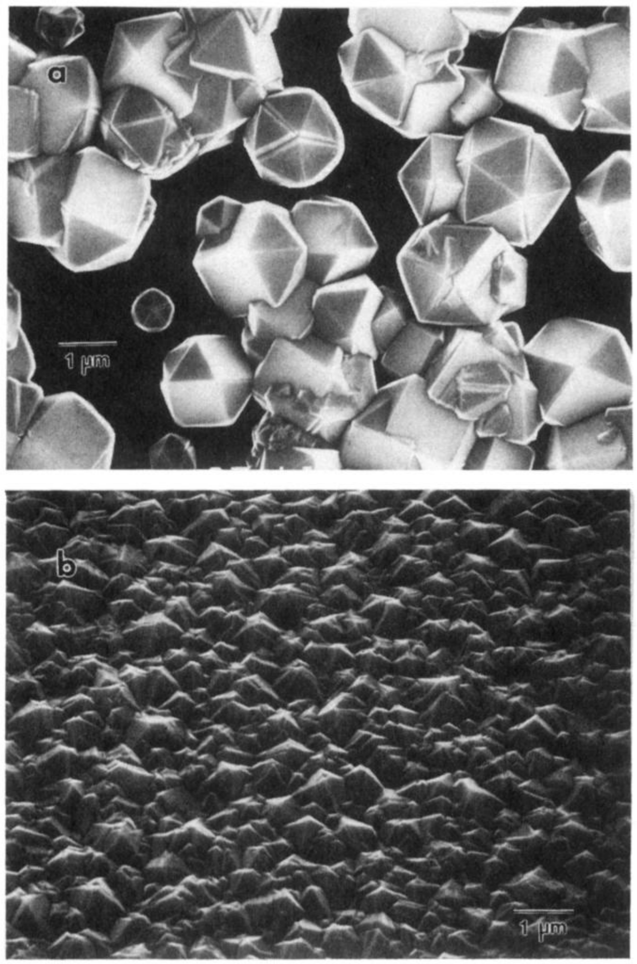

FIG. 3. SEM micrographs of samples grown under various pretreatments: (a) silicon wafer scratched with 0.25-μm diamond powder and (b) pristine silicon wafer biased on a (2% methane)-in-hydrogen plasma at -250 V for 1 h.

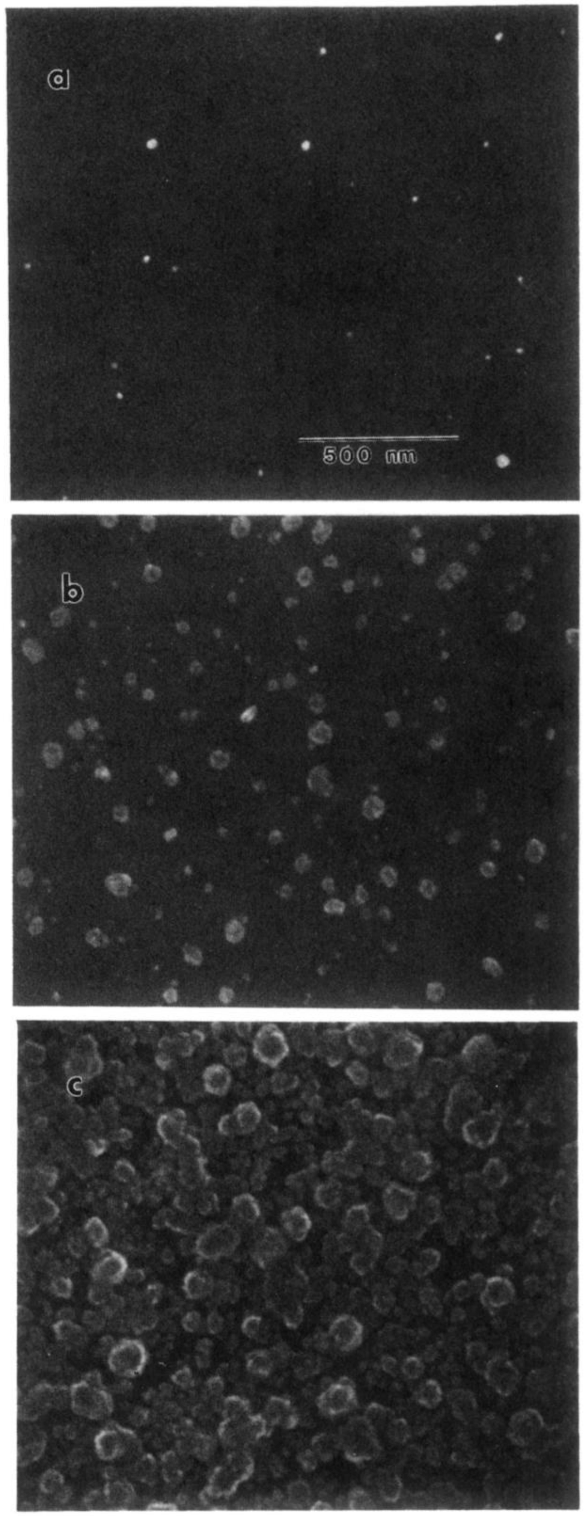

FIG. 9. SEM micrograph of the bias pretreatment after (a) 1.0 h, (b) 1.5 h, and (c) 2.0 h. Magnification scale is the same for all three.